



BASQUE CENTRE
FOR CLIMATE CHANGE
Klima Aldaketa Ikergai

**The Uniform World Model:
A Methodology for Predicting
the Health Impacts of Air Pollution**

Joseph V. Spadaro

December 2011

BC3 WORKING PAPER SERIES

2011-12

The Basque Centre for Climate Change (BC3) is a Research Centre based in the Basque Country, which aims at contributing to long-term research on the causes and consequences of Climate Change in order to foster the creation of knowledge in this multidisciplinary science.

The BC3 promotes a highly-qualified team of researchers with the primary objective of achieving excellence in research, training and dissemination. The Scientific Plan of BC3 is led by the Scientific Director, Prof. Anil Markandya.

The core research avenues are:

- Adaptation to and the impacts of climate change
- Measures to mitigate the amount of climate change experienced
- International Dimensions of Climate Policy
- Developing and supporting research that informs climate policy in the Basque Country

See www.bc3research.org for further details.

The BC3 Working Paper Series is available on the internet at http://www.bc3research.org/lits_publications.html

Enquiries (Regarding the BC3 Working Paper Series):

Roger Fouquet

Email: roger.fouquet@bc3research.org

www.bc3research.org

The opinions expressed in this working paper do not necessarily reflect the position of Basque Centre for Climate Change (BC3) as a whole.

Note: If printed, please remember to print on both sides. Also, perhaps try two pages on one side.

The Uniform World Model

A Methodology for Predicting the Health Impacts of Air Pollution

Joseph V. Spadaro¹

Throughout history, technological development and economic growth has led to greater prosperity and overall standard of living for many people in society. However, along with the benefits of economic development comes the social responsibility of minimizing the mortality and morbidity health impacts associated with human activities, safeguarding ecosystems, protecting world cultural heritage and preventing integrity and amenity losses of man-made environments. Effects are often irreversible, extend way beyond national borders and can occur over a long time lag. At current pollutant levels, the monetized impacts carry a significant burden to society, on the order of few percent of a country's GDP, and upwards to 10% of GDP for countries in transition. A recent study for the European Union found that the aggregate damage burden from industrial air pollution alone costs every man, woman and child between 200 and 330 € a year, of which CO₂ emissions contributed 40 to 60% (EEA 2011).

In a sustainable world, an assessment of the environmental impacts (and damage costs) imposed by man's decisions on present and future generations is necessary when addressing the cost effectiveness of local and national policy options that aim at improving air quality and reducing greenhouse gas emissions. The aim of this paper is to present a methodology for calculating such adverse public health outcomes arising from exposure to routine atmospheric pollutant emissions using a simplified methodology, referred to as the Uniform World Model (UWM). The UWM clearly identifies the most relevant factors of the analysis, is easy to implement and requires only a few key input parameters that are easily obtained by the analyst, even to someone living in a developing country. The UWM is exact in the limit all parameters are uniformly distributed, due to mass conservation.

The current approach can be applied to elevated and mobile sources. Its robustness has been validated (typical deviations are well within the $\pm 50\%$ range) by comparison with much more detailed air quality and environmental impact assessment models, such as ISC3, CALPUFF, EMEP and GAINS. Several comparisons illustrating the wide range of applicability of the UWM are presented in the paper, including estimation of mean concentrations at the local, country and continental level and calculation of local and country level intake factors and marginal damage costs of primary particulate matter and inorganic secondary aerosols. Relationships are also provided for computing spatial concentrations profiles and cumulative impact or damage cost distributions. Assessments cover sources located in the USA, Europe, East Asia (China) and South Asia (India).

Keywords: Air Pollution, Urban Air Quality, Particulate Matter, Air Quality Modeling,
Health Impact Assessment, Loss of Life Expectancy, Damage Costs of Air Pollution.

JEL Classification: C63, I15, O13, O44 and Q53

Cite as: Spadaro, JV. (2011) The Uniform World Model: A methodology for Predicting the Health Impacts of Air Pollution. BC3 Working Paper Series 2011-12. Basque Centre for Climate Change (BC3). Bilbao, Spain.

¹ Basque Centre for Climate Change (BC3). Alameda Urquijo, 4 – 4^o, 48008 Bilbao, Spain. Corresponding author
E-mail: joseph.spadaro@bc3research.org.

1. Introduction

The epidemiological literature, over the past two decades, has reported extensively on the link between adverse health effects and pollutant ambient concentration increases from human activity (HEI, 2010). The evidence presented so far has often shown a statistically significant association between respirable particulate matter, PM, (usually, identified in studies as PM_{2.5} or PM₁₀) and unintended health impacts. Taking into consideration the environmental and health consequences of pollution has therefore become a key component in energy forecasting analyses, whether the scope of the planning is at the local, regional or global-level.

An Environmental Impact Assessment (EIA) necessitates inputs from a well detailed multi-disciplinary database of historical and projected values regarding source technical specifications, environmental loadings, demographics, geographical and weather data, population health statistics, exposure risks (concentration-response functions, CRF, from epidemiological studies) and social costs. The necessary information is often limited; this is especially true in developing countries. This lack of data contributes to the uncertainty of the final result, apart from input parameter variability (geographic and physio-chemical variance, urban vs. rural dispersion, low vs. tall stack, diurnal vs. seasonal vs. long-term changes, background ambient concentration levels, and so forth), choice of future scenario (will there be a cancer cure by 2050?) and analyst mistakes. Some of these uncertainties/variances can be addressed using a formal statistical analysis, while others cannot (Rabl and Spadaro, 1999; Spadaro and Rabl, 2008).

The aim of this write-up is to present a methodology for calculating the adverse public health outcomes from exposure to routine atmospheric pollutant emissions due to ground-level or elevated sources using a simplified approach that identifies the most significant parameters of the analysis (transparent and not “black-box” as are most often EIA software tools), that is easy to implement and that requires a limited number of input data that are easily obtained by the analyst. The current approach can be used to model isolated (point), area or mobile releases. The tradeoff for simplicity, however, should not compromise the accuracy and validity of the output estimates, rendering them useless inputs to other models or deemed insufficiently robust for inclusion in policymaking debates. The methodology presented here will be referred to as the Uniform World Model (UWM). Validation of this method is by way of output comparison with more established and detailed impact assessment software, currently used in air quality analysis. The UWM can also be used as a “sanity” check, comparing its estimates with predictions from detailed EIA assessments and checking the results for coherence. These inconsistencies in predictions, among other reasons, may arise because of erroneous specifications of technical, demographic or environmental database information, which might be the result of entry errors or analyst misinterpretations.

2. Health Impacts if Air Pollution

Consider a source emitting a pollutant p at the rate Q_p . p is called a primary pollutant because it is emitted directly into the air at the source location. Those pollutants that subsequently form in the atmosphere due to chemical transformation are called secondary, s , species; their formation rate is related to Q_p , the atmospheric removal rate of p due to dry and wet deposition (and radioactive decay) and chemical transformation rate, p to s conversion. Deposition rates depend on numerous factors, including weather conditions (precipitation rate, for example), time of day or season of year, vegetation cover (land use) and particle size ($PM_{2.5}$ has a longer atmospheric residence than PM_{10} , for example). In the case of sulfur dioxide, SO_2 , the transformation rate is typically 1% per hour. Health impacts from direct exposure (inhalation) to primary or secondary pollutants are estimated using the relationship shown in Eq.1. The second equality follows from the assumption that, typically, the product $\beta (C-C_0) \ll 1$. This inequality is certainly true for the current levels of pollution that are observed in the US and Europe. For Asia, on the other hand, the product $\beta (C-C_0)$ is on the order of 1.

$$Impact = Impact_0 e^{\beta (C-C_0)} \approx Impact_0 [1 + \beta (C - C_0)] \quad (1)$$

C and C_0 are, respectively, the ambient concentrations including and excluding the emission source contribution. For particulate matter (PM), C is not a function of background ambient concentration. Hence, C is proportional to the emission rate Q_p (although for some pollutants there may be a lag time between emission and steady state ambient concentration; this is the case for mercury, for example). For SO_2 and nitrogen oxides, NO_x , their concentrations will be influenced by the pre-existing ambient levels of these pollutants, their derived secondary species (among which are ozone and gaseous/particulate aerosols) and other background compounds (ammonia). C is a function of distance from source, emission rate and other source characteristics, weather conditions and land use and topography (natural and man-made obstacles). β is the health risk factor determined from epidemiological studies; it has units of % change in health impact per unit concentration change ($\mu g/m^3$). Each health outcome has an associated value of β (0.6% per $\mu g/m^3$ $PM_{2.5}$ for long-term mortality effects, as per Pope et al., 2002). Impact has units of health cases per year for a concentration C , while $Impact_0$ is the “background” rate for a concentration C_0 . The total (aggregated) impact is the sum of Impacts across the entire domain area of the analysis.

The value of C , as mentioned previously, is a function of the downwind distance from the emitting source (what is referred to as the source-receptor distance). Concentrations are estimated using dispersion models, which vary greatly in complexity and can take into account many different atmospheric characteristics, including 3-dimensional dispersion (horizontal and across multiple vertical layers), time dependence and chemical transformation (Seinfeld and Pandis, 1998; Zannetti 1990). At the “local” scale, within 50 kilometers of the source, steady state Gaussian models have

traditionally been used (e.g., the Industrial Source Complex, ISC, Model; EPA 1995). The basic premise is that once the pollutant is emitted into the atmosphere, the vertical and horizontal concentration profiles may be adequately represented as two independent Normal distributions, each characterized by its own standard deviation or sigma parameter (Fig.1). While the plume rises across the atmosphere, driven by inertia and buoyancy forces, it continually spreads along the downwind (x) and crosswind (y) directions because of turbulent entrainment. In deriving the concentration governing equations, pollutant removal from dry and wet deposition and chemical transformation is considered unimportant, as is the spatial (horizontal) variation in weather conditions across the local domain (10,000 km² area). The Gaussian model is considered most accurate for predicting long term or annual concentrations, rather than estimates for episodic events.

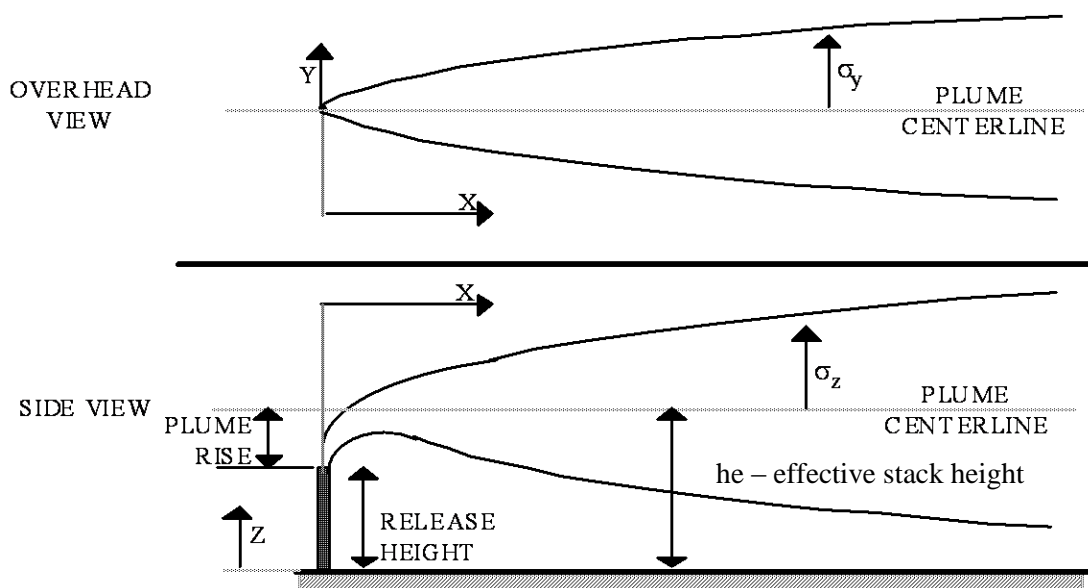


Fig.1. Gaussian plume in a wind-oriented (x-direction) coordinate system

The influence of pollutant removal and transformation beyond 50 km cannot be overlooked. Accounting for these effects leads to more complex dispersion algorithms, which must attempt to capture more faithfully atmospheric variations in time and space (horizontal and vertical directions). Weather changes, whether they occur on a daily or seasonal time-scale, can have a profound impact on concentrations. A rainstorm can washout the bulk of a pollutant in the plume, while NOx transformation is strongly influenced by ambient temperature, sunlight and the presence of other compounds in the air, namely ammonia (Zhou et al., 2003). Health impacts depend on the amount of pollutant intake, which may enter the body via different routes of exposure, including inhalation or ingestion of contaminated foodstuff. Some pollutants remain in the air for several days and can expose a large fraction of the “regional” population (1000’s km downstream of the source); whereas others have an environmental residency time on the order of years, decades (or even longer), and thus have a global range (carbon dioxide, methane, mercury, for example) or even an inter-generational

impact (heavy metals, radionuclides). For the heavy metals, the inhalation route only contributes a few percent of the total exposure.

There are numerous long range (transboundary) transport models, including the Windrose Trajectory Model of ExternE (Krewitt et al., 1995), EMEP (the official model used for policy decisions about trans-boundary air pollution in Europe <http://www.emep.int>) and CALPUFF (Scire et al., 2000). Developed by the US Environmental Protection Agency (EPA), CALPUFF is a Lagrangian puff model (Zannetti 1990). It simulates mass transport as pollutant puffs that are released into the air at regular intervals. Dispersion is based on Gaussian diffusion, along with pollutant removal by dry and wet deposition and chemical transformation. The ambient wind flow carries the puffs downwind from the source. The prevailing wind direction and wind speed varies with time and space, unlike the Gaussian model which assumes a horizontally homogeneous wind field. At a particular location in the domain (receptor site), the pollutant concentration is a weighted mean of all puffs crossing that point. CALPUFF can be used to model both primary and secondary pollutants.

The USEPA has compared concentration estimates from CALPUFF with ISC, EPA's widely used default model for regulatory applications, until it was replaced by AERMOD (EPA 1998a). The EPA has also compared CALPUFF concentration estimates with tracer gas concentrations from two short-term field experiments (EPA 1998b). The conclusions from these studies are summarized below. The EPA findings suggest that a factor of two between modeled and measured concentrations is to be expected. This conclusion is in complete agreement with the population-total exposure uncertainty analysis carried out by Spadaro and Rabl (2005), who in their analysis recommended a geometric standard deviation, σ_g , of 1.2 for a large city, 1.9 for a rural site and a value of 1.5 for the typical location. The high to low ratio for the 68% confidence interval is 1.5^2 , or a factor of 2.25.

Box 1. “Overall trends have been noted in the percentage difference comparisons in simulated concentration values between CALPUFF and ISC3. For taller point sources, there is a trend toward higher concentrations being simulated by CALPUFF in comparison to ISC3. For annual averages, the closer a receptor is to the source and the taller the stack, the greater the chance that the CALPUFF concentration values will be higher than those simulated by ISC3. At the more distant downwind receptor rings, the bias changes direction from CALPUFF yielding higher concentrations, to CALPUFF yielding relatively lower concentrations and sometimes these concentrations are lower than their respective ISC3 counterpart.”

Source: A Comparison of CALPUFF with ISC3 (EPA 1998a)

Box 2. “The performance of the CALPUFF atmospheric dispersion model for two field tracer experiments is summarized. The first tracer experiment was in 1975 at Savannah River Laboratory and the second was in 1980 in the central United States. Both experiments examined long-range transport of an inert tracer material. The results generally were encouraging, with the simulated results within a factor of two of the observed data for the statistical measures presented in the report. However, there is not a consistent pattern of over- or under-estimation relative to the observations.”

Source: A Comparison of CALPUFF Modeling Results to Two Tracer Field experiments (EPA 1998b)

Eqn.1 is oftentimes recast in a slightly different format, as indicated in Eqn.2 below.

$$I = \sum_j (Impact_j - Impact_0) \approx \sum_j Impact_0 \beta (C_j - C_0) \quad (2a)$$

$$I \approx \sum_j \left[\frac{Impact_0 \beta}{Pop} \right]_j \Delta C_j Pop_j = \sum_j S_{CR,j} \Delta C_j Pop_j = S_{CR} \sum_j \Delta C_j Pop_j \quad (2b)$$

I is the total incremental impact (annual events or cases) due to emission rate Q, summed over all gridded receptors Pop_j affected by the pollutant in question (the sum is replaced by an integral for a continuous distribution). Impact₀ is the population weighted “baseline” impact rate; that is, the annual cases of mortality or morbidity that are observed at concentration level C₀ among the population at risk. ΔC_j is the incremental concentration, above background value C₀, due to emission rate Q at grid point j. S_{CR} is the concentration-response function slope, derived from epidemiological studies, with units additional annual cases per person per unit concentration (annual events per [pers – μg/m³]).

In writing the final equality in Eqn.2b, it is assumed that the CRF has a constant value across the entire impact domain for all possible concentration increments above background (S_{CR} is not a function of C_j). The assumption that is usually made in EIA studies is that the CRF is linear, with slope S_{CR} and without a threshold at zero concentration. This might be the case for background pollutant concentrations prevailing in the US and Europe (Order of 10 μg/m³), but may not hold true for the range of concentrations that are typically observed in Asian countries, which can range between three and ten times (or even more, Order of 100 μg/m³) higher than those measured in the West (HEI 2010). Extrapolating β values beyond the concentration range of the original epidemiological studies could lead to erroneous conclusions – likely over-estimates. Cohen et al., (2004) have considered this issue and have proposed alternative CRFs for cardiopulmonary mortality

(Fig.2). Pope et al., (2009) and (2011) and Kalantzi et al., (2011) provide further evidence of the non-linear shape of CRFs for cause-specific mortality and for hospital admissions, respectively, at high ambient concentrations (Fig.3).

Finally, to get the damage cost D_i (cost per year) for a specific health endpoint i , the impact is multiplied by the appropriate unit cost factor $U_{cost,i}$ for that disease (cost per health event). Unit costs account for direct and indirect costs and welfare loss. In Eqn.3, a constant (mean) unit cost factor is applied across the entire impact area of the analysis. The total damage cost D is the sum of the costs of the individual health endpoints. D/Q is the damage cost per unit emission or the marginal damage cost, with typical units of \$/kg or €/kg.

$$D = \sum_i D_i = \sum_i \left[S_{CR,i} U_{cost,i} \sum_j \Delta C_j Pop_j \right] \quad (3)$$

3. Uniform World Model Methodology

The Uniform World Model (UWM) is a solution to Eqn.3 for a set of simplifying conditions. For continuous concentration and receptor distributions, the summation in Eqn.3 is replaced by a surface integral covering the impact area of the analysis (usually, 1000's of km downwind of the source).

$$D = \sum_i D_i = \sum_i \left[S_{CR,i} U_{cost,i} \int_{\text{Impact Area}} \Delta C(Q_p, \bar{r}) \rho(\bar{r}) d\bar{r} \right] \quad (4)$$

ΔC is the incremental change in background concentration ($\mu\text{g}/\text{m}^3$) of either the primary or the secondary pollutant due to a primary pollutant air discharge rate Q_p ($\mu\text{g}/\text{s}$) at location \bar{r} and $\rho(\bar{r})$ is the receptor density (persons per m^2).

Simplifying assumptions

(a1) Local and background receptor distributions (pers/ km^2) are different, but people are uniformly spread across their respective domains.

$$\rho(\bar{r}) = \rho_{eff} = \left[f_{loc} \left(\frac{\rho_{loc}}{\rho_{back}} \right) + (1 - f_{loc}) \right] \rho_{back} \quad (5a)$$

f_{loc} is the local share of the UWM impact or damage cost (unit-less). Values for particulate matter range between 5% and 20%, with 15% being a typical value for PM. ρ_{loc} and ρ_{back} represent the local (< 50 km) and background receptor densities, respectively. Together they define the weighted mean ρ_{eff} . Another expression for computing ρ_{eff} (for 100m stacks) is given in Eqn.5b.

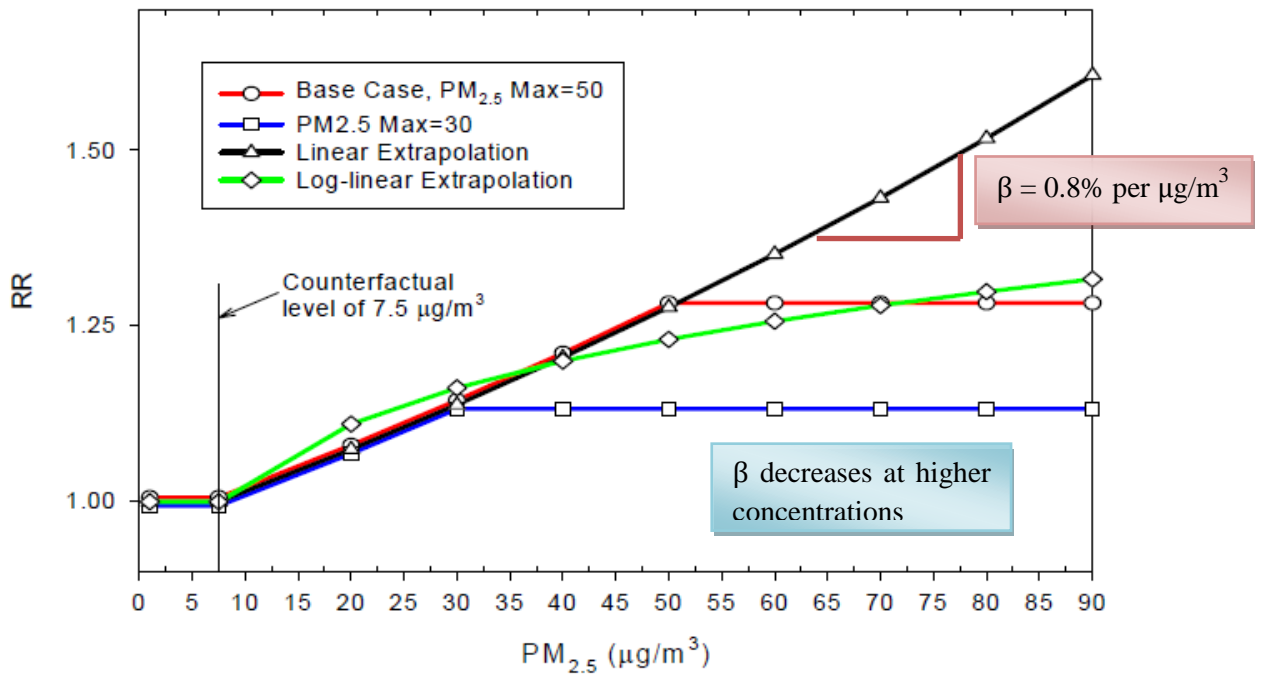


Fig.2. Alternative CRFs representations for cardiopulmonary mortality (Cohen et al., 2004); RR stands for relative risk (compared to background or counterfactual value).

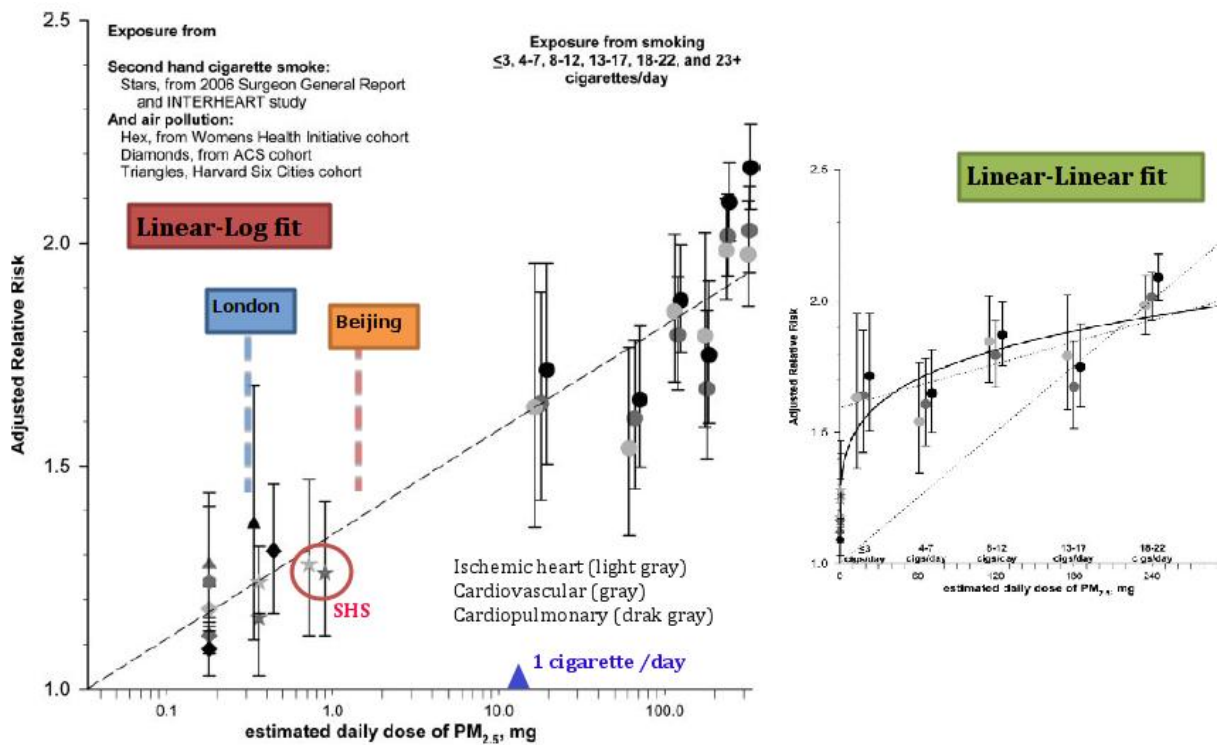


Fig.3. Adjusted relative risks (relative to never smokers or background) for cigarette smoking, second-hand-smoking (SHS) and air pollution (adapted from Pope et al., 2009).

$$\rho(\bar{r}) = \rho_{eff} = \left[0.7972 \left(\frac{\rho_{loc}}{\rho_{back}} \right)^{0.7912} \right] \rho_{back} \quad (5b)$$

Values from Eqns.5a and 5b can be averaged to obtain a third estimate.

In order to capture at least 95% of the total damage cost, the UWM assumes a circular impact domain with typical radius ranging from 500 km for a pollutant source located near a large city and up to 1,000 km for a rural site (Fig.4). For secondary species, such as particulate aerosols, the impact range extends from 1,000 to 1,500 km (Fig.5), independent of source location and stack parameters (such as physical stack height). As the local wind field carries primary pollutants away from the source, secondary species are formed through chemical interactions with other atmospheric compounds, and hence, their impact reach extends further downstream. For Europe (EU-27), the mean value of ρ_{back} is 112 pers/km², and for China a value of 231 pers/km² is recommended.

(a2) At any point \bar{r} , along the horizontal plane at ground-level, the ratio of pollutant removal flux $M(Q_p, \bar{r})$ and $\Delta C(Q_p, \bar{r})$ is constant (i.e., homogeneous atmosphere).

$$M(Q_p, \bar{r}) = k \times \Delta C(Q_p, \bar{r}) \quad (5c)$$

$M(Q_p, \bar{r})$ has units of $\mu\text{g/s}$ per unit of surface area (m^2). For primary pollutants, the proportionality constant k is the pollutant removal or depletion velocity. k has units of m/s and accounts for all removal pathways, including dry and wet deposition, chemical transformation and radioactive decay. For secondary species, k is an effective depletion velocity. It is the product of the primary and secondary removal velocities divided by the primary-to-secondary transformation velocity, which links the formation of the secondary contaminant to the primary pollutant emission rate Q_p (Spadaro 1999). Typical ranges of k are 0.6 to 2 cm/s for PM_{10} , 0.4 to 0.9 for $\text{PM}_{2.5}$, 0.7 to 2 cm/s for SO_2 , 0.4 to 2.3 cm/s for NO_x , 1.7 to 3.3 cm/s for ammonium sulfates ($(\text{NH}_4)_2\text{SO}_4$) and 0.7 to 1.5 cm/s for ammonium nitrates (NH_4NO_3). k is strongly influenced by precipitation rate (wet deposition). For instance, the value of k for Northern Brazil (near the Amazon Forrest) is 2.9 cm/s for PM_{10} , whereas for Southern Brazil the depletion velocity is less than half that value, or 1.3 cm/s .

Different methods for computing k have been proposed (Spadaro 1999). One approach is to carry out a regression analysis of measured or modeled concentration estimates as a function of downwind distance (Eqn.10). In other instances, the depletion velocity can be estimated using the pollutant's atmospheric residence time (time needed for a pollutant's concentration to decrease by $1/e$ of its original value or the expectation (mean) value of time before a pollutant is removed from the air) or, more formally, by using an atmospheric removal rate equation. Yet, other times, existing values may be transferred to another location based on similarities between two sites or deduced from existing

results after adjusting for differences in meteorology (precipitation), topography and land cover between reference and target locations. For situations in which there are no available data, preliminary default values of 1 cm/s may be assumed for PM_{10} , 0.67 cm/s for $PM_{2.5}$ (current experience indicates that the ratio of PM_{10} to $PM_{2.5}$ depletion velocities is about 1.5), 2 cm/s for ammonium sulfates and 1 cm/s for ammonium nitrates.

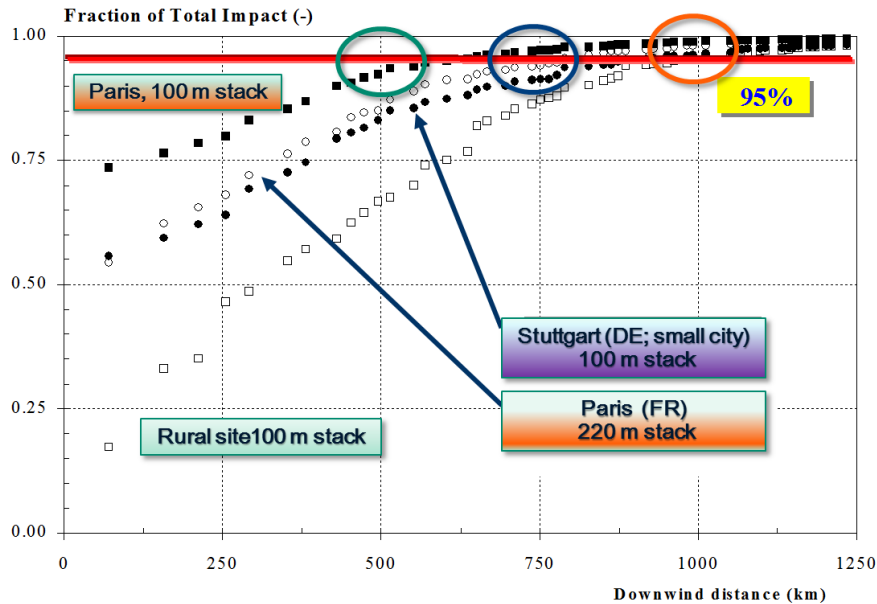


Fig.4. PM_{10} cumulative impact distribution

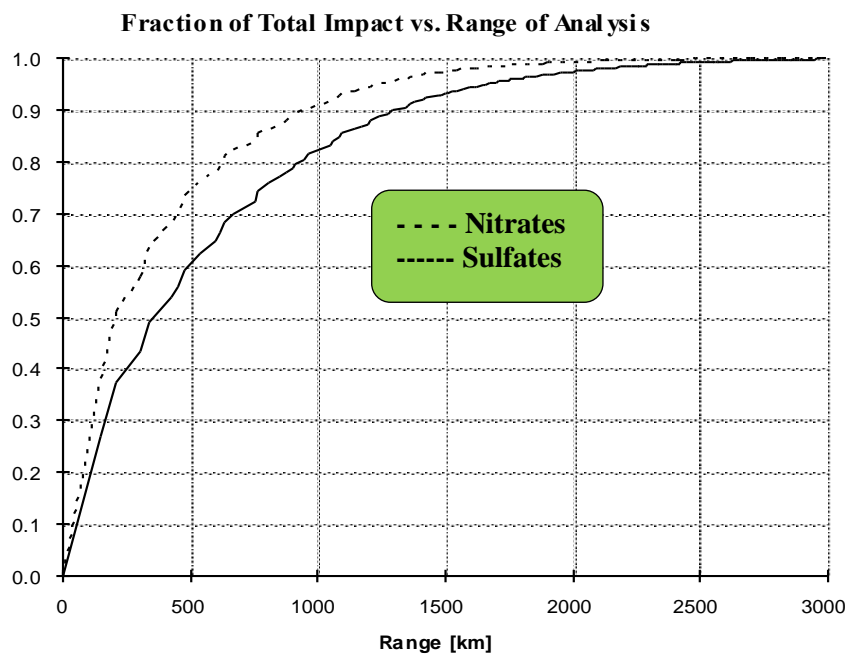


Fig.5. Secondary pollutant cumulative impact distribution for a source located in France (concentration data from EMEP; uniform receptor density; Curtiss and Rabl, 1996)

The Uniform World Model mean incremental concentration estimate \bar{C}_{UWM} is given by Eqn.6 below.

$$\bar{C}_{UWM} = \frac{1}{A} \int_{\text{Impact Area}} \Delta C(Q_p, \bar{r}) d\bar{r} = \frac{1}{A} \int_{\text{Impact Area}} \frac{M(Q_p, \bar{r})}{k} d\bar{r} = \frac{Q_p}{A \times k} \quad (6)$$

A is the circular impact domain area in m², with radius ranging between 1,000 and 1,500 km for primary and 1,500 to 2,000 km for secondary pollutants (Fig. 5). The final equality follows from mass conservation when steady state conditions prevail. For secondary particulate matter (SPM), Q_p is the precursor pollutant emission rate, namely, SO₂ for sulfates and NO_x for nitrates.

The pollutant intake factor iF (dimensionless) is another metric that is often used in life-cycle analyses to quantify human exposure to chemicals. The intake factor is the fraction of the pollutant that is emitted into the environment and then enters the human body via different routes of exposure, including inhalation, water use, contaminated foodstuff consumption (meats, fish, vegetables, etc.) soil ingestion, dermal contact and possibly by external irradiation. In the case of air pollution, inhalation is the exposure pathway for a chemical to enter the human body. Assuming a population weighted mean daily breathing rate B_R equal to 13 m³ per person (EPA 2011), the intake factor for a population of N_{pers} individuals (men, women and children) is estimated using Eqn.7.

$$iF = \frac{\bar{C}_{UWM} N_{pers} B_R}{Q_p} = \frac{N_{pers} B_R}{A \times k} = \frac{\rho_{eff} B_R}{k} \quad (7)$$

ρ is the ordinary population density in pers/m² (i.e., not weighted as in Eqn.5a). The absorbed dose is less than the intake dose. For dioxins, as an example, only 50% of the mass entering the human body will eventually be absorbed. For cadmium, 50% and 5%, respectively, will be absorbed in the human body via the inhalation and ingestion pathways. The absorption rate and primary pathways for health risks are chemical dependent.

Substituting Eqns.5a (or 5b) and 5c into Eqn.4 and realizing that the surface area integral of the pollutant removal flux is equal to the source emission rate from mass conservation at steady state, yields the “basic” UWM annual damage cost estimate D_{UWM} for a pollutant emission rate Q_p (annual damage cost, aggregated over all health endpoints i). D_{UWM}/Q_p is the uniform world model marginal damage cost, d_{UWM} (cost per kg emission).

$$D_{UWM} = \left(\frac{Q_p \rho_{eff}}{k} \right) \sum_i [S_{CR,i} U_{cost,i}] \quad (8a)$$

$$d_{UWM} = \frac{D_{UWM}}{Q_p} = \left(\frac{\rho_{eff}}{k} \right) \sum_i [S_{CR,i} U_{cost,i}] \quad (8b)$$

In Eqn.9, the “basic” UWM relation has been modified by the two multipliers: S_{sh} and S_{ct} . Coefficient S_{sh} is a scaling factor used to improve the accuracy of the UWM estimate (Eqn.8) by taking into consideration the physical stack or release height (Fig.1) and the source location; hence, differentiating between large and small cities, between urban and rural locations, or between tall and short stacks. Recommendations for S_{sh} and S_{ct} are summarized in Tab.1 (also see Fig.6). Eqn.9 is most appropriate for estimating site-specific damage costs (individual sources), whereas Eqn.8 is most appropriate for an analysis at the regional- or country-level (see European assessment below).

$$D_{UWM}^{Improved} = S_{sh} \times S_{ct} \times D_{UWM} = S_{sh} S_{ct} \left(\frac{Q_p \rho_{eff}}{k} \right) \sum_i [S_{CR,i} U_{cost,i}] \quad (9)$$

The parameter S_{ct} is a scaling factor that accounts for non-linearities in chemical reactions, an important issue that comes up in the transformation of non-marginal emissions of nitrogen oxides (Zhou et al., 2003). Both nitrogen and sulfur compete for the ammonia that is present in the atmosphere to neutralize nitric and sulfuric acid, but ammonia preferentially neutralizes sulfates over nitrates. Moreover, unlike sulfates, nitrate formation is reversible; the equilibrium between nitric acid, ammonium nitrate and ammonia can shift depending on atmospheric ammonia availability and ambient temperature. During summer months, for instance, higher temperatures limit nitrate formation considerably (see West et al., 1999 and Table 2 in Zhou et al., 2003, for example). Hence, for non-marginal NOx emissions, S_{ct} is assigned a value between 0.25 and 0.5 (recommended). For all other pollutants and marginal NOx emissions, generally, a change in background ammonia concentration has no appreciable effect on other pollutant concentrations, thus S_{ct} is set to unity. The scalars S_{sh} and S_{ct} can be used to modify the expressions for the mean UWM concentration (Eqn.6) and the pollutant intake factor (Eqn.7) to account for stack height variability, source location and chemical transformation non-linearities.

Tab.1. Multiplier coefficients for use in Eqn.9

Pollutant	Site characterization	S_{sh} [-]	S_{ct} [-]
PM ₁₀ , SO ₂ and NOx	Rural, $\left(\frac{\rho_{loc}}{\rho_{back}}\right) < 2$	<ul style="list-style-type: none"> 1.5 for hs = 25 m 0.9 for hs = 225 m 2 for transport 	1
	Small city, $\left(\frac{\rho_{loc}}{\rho_{back}}\right) < 6$	<ul style="list-style-type: none"> 1.3 for hs = 25 m 0.8 for hs = 225 m 10-15 for transport 	
	Medium city, $\left(\frac{\rho_{loc}}{\rho_{back}}\right) < 10$	<ul style="list-style-type: none"> 1.4 for hs = 25 m 0.7 for hs = 225 m 20-40 for transport 	
	Large city, $\left(\frac{\rho_{loc}}{\rho_{back}}\right) > 10$	<ul style="list-style-type: none"> 1.6 for hs = 25 m 0.6 for hs = 225 m Up to 100 for transport 	
Sulfates		<ul style="list-style-type: none"> ± 30% (see Fig.6) weak dependence on stack height and site 	1
Nitrates		<ul style="list-style-type: none"> ± 40% (see Fig.6) weak dependence on stack height and site; greater variability than sulfates due to non-linear chemistry 	<ul style="list-style-type: none"> For non-marginal emissions: 0.25 to 0.5 (0.5 recommended) For marginal emissions: ≈1

Footnotes – hs is the physical stack height (m)

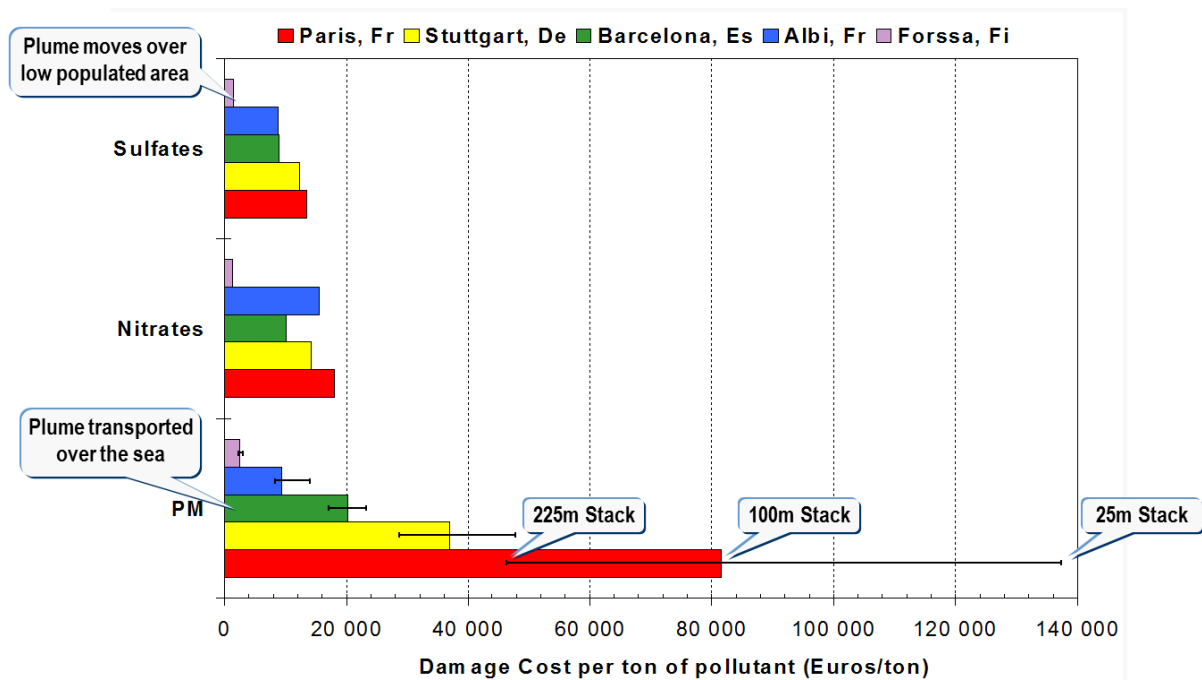


Fig.6. Variability of damage costs with geographical location.

For a uniform (k constant) and well-mixed atmosphere (concentration is vertically uniform across the planetary boundary layer), characterized by a constant mixing height h_{mix} and a horizontally homogeneous windrose field (constant wind speed, blowing with equal probability in all directions), the steady state incremental concentration C due to an emission rate Q_p at downwind distance \bar{r} is given by Eqn.10a and Eqn.10b for primary (subscript “p”) and secondary (subscript “s”) pollutants, respectively.

Primary pollutant p (Q_p emission rate)

$$C_p(r) = \frac{Q_p}{2 \pi u h_{\text{mix}}} \frac{1}{r} e^{-\frac{k_p}{u h_{\text{mix}}} r} = \frac{a_p}{r} e^{-\lambda_p r} \quad (10a)$$

Secondary pollutant s (equivalent emission rate $Q_s = \frac{k_{ct}}{k_p} Q_p$)

$$C_s(r) = \frac{Q_p}{2 \pi u h_{\text{mix}}} \frac{1}{r} \left(\frac{k_{ct}}{k_s - k_p} \right) \left[e^{-\frac{k_p}{u h_{\text{mix}}} r} - e^{-\frac{k_s}{u h_{\text{mix}}} r} \right] = \frac{a_s}{r} \left[e^{-\lambda_p r} - e^{-\lambda_s r} \right] \quad (10b)$$

h_{mix} is the mixing layer depth, the turbulent boundary layer above the ground (lower troposphere) where mass and energy transport and chemical transformation occur (planetary boundary layer, PBL). Within the PBL, the air is influenced by interactions at the earth’s surface such as mechanical and thermal forcing and surface topography. h_{mix} varies with time of day/year and as a function of solar radiation and atmospheric turbulence, increasing from morning to late afternoon (Fig.7). Mixing height has a lognormal distribution. Values usually range between 100 and 2000 meters, with a typical mean estimate of 800 m and a coefficient of variability of 50%, or more. Measurements and diagnostic estimates of h_{mix} can differ by as much as an order of magnitude, when compared to each other.

u is the mean wind speed (m/s); a typical planetary boundary layer value is 5 m/s. The product $u \times h_{\text{mix}}$ is the pollutant dilution rate or ventilation index m_R (m^2/s). k_p (k_s) is the primary (secondary) pollutant depletion velocity (m/s). k_{ct} is the primary to secondary chemical transformation velocity (transformation rate τ_R multiplied by h_{mix}). For SO_2 to sulfate conversion, as an example, a typical estimate for the transformation rate is 1% per hour, but literature estimates can vary widely between 0.2% and 7%, depending on atmospheric photochemical activity, air temperature and humidity, and time of day or day of year (Lee and Watkiss 1998, Luria et al., 2001, Khoder 2002, Miyakawa et al., 2007). The NO_x transformation rate to particulate (ammonium nitrate) + gaseous (nitric acid) species is lower than the SO_2 conversion rate (Khoder 2002). Transformation rates follow a lognormal distribution, as do air concentrations (geometric standard deviation between 1.5 and 2). The ratio k_{ct} to k_p is equal to the product of the pollutant atmospheric residence time τ_t and transformation rate τ_R .

The term $\frac{k}{u h_{mix}}$ is the pollutant decay factor λ ; it represents, close to the source, the rate at which the pollutant concentration decreases with downwind distance (% per km).

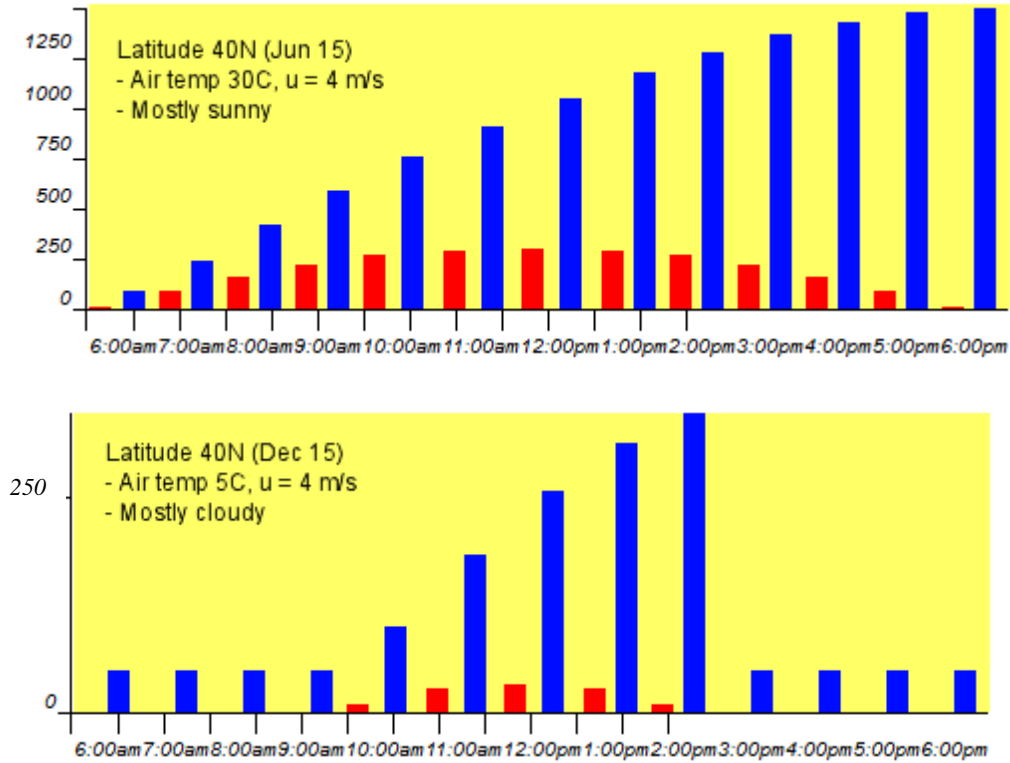


Fig.7. Surface heat flux (red bars, W/m²) and daytime atmospheric mixing depth (blue bars, m) for a rural site. (Ref: Luhar 1998)

For a primary pollutant, the mean incremental concentration $\bar{C}_p(R_o)$ over $r = 0$ and $r = R_o$ is obtained by integrating Eqn.10a (the impact area A is πR_o^2). For the local domain ($A=10^4$ km²), R_o is 56 km.

$$\bar{C}_p(R_o) = \frac{1}{A} \int_0^{R_o} 2 \pi r C_p(r) dr = \frac{Q_p}{\pi k_p R_o^2} \left[1 - e^{-\frac{k_p R_o}{u h_{mix}}} \right] \quad (11)$$

The exponential inside the square brackets is the fraction of pollutant mass Q_p remaining in the plume at downwind distance R_o . In the limit of large R_o , $\bar{C}_p(R_o)$ reduces to \bar{C}_{UWM} (Eqn.6). The factors S_{sh} and S_{ct} in Tab.1 can provide improved mean concentration estimates. Eqns.10a and 11 are plotted in Figs.8 and 9, respectively, as a function of downwind distance r for different dilution rates m_R and depletion velocities k_p . As can be seen in these figures, near the source and for mid-range distances the dilution rate is the contributing factor for decreasing pollutant concentrations. The depletion velocity influence on concentration is negligible near the source, but increases significantly with downwind distance; eventually, pollutant removal becomes the leading cause for changes in concentration. Higher dilution rates, at large distances, lead to higher air concentrations (Fig.8)

because the relative influence of pollutant removal, compared to dilution, is diminished, that is the pollutant remains in the air for a longer period of time before it is removed.

In Fig.10, the mean concentration calculated from Eqn.11 is compared with results obtained using the ISC model of the USEPA (EPA 1995) for an urban source, located near Paris (France), of varying physical stack heights (h_s). Emission rate Q_p is 1000 tonnes per year (1 kt/yr) and domain size R_o is 56 km, corresponding to an area of 10,000 km². For tall stacks (greater than 250 m), the agreement is much better because the well-mixed atmosphere hypothesis, across the local impact range, is more realistic than for cases of low stacks. A regression fit of ISC mean concentrations and stack heights provides a functional relation for the parameter S_{sh} (Eqn.12). Specific values will depend on prevailing flue gas exhaust conditions, the two extremes being high exhaust flow rate at high temperature (largest plume rise) and low exhaust flow rate at low temperature (smallest plume rise).

$$S_{sh} = \frac{20}{h_s^{0.49}} \text{ (small plume rise); } \quad S_{sh} = \frac{14}{h_s^{0.54}} \text{ (large plume rise) } \quad \langle \text{urban source} \rangle \quad (12)$$

For a primary pollutant, Eqn.10a can be used to derive the uniform world model damage cost distribution function $D_{UWM,p}(r)$ for downwind distance r (Eqn.13), whereas Eqn.11 can be used to derive the cumulative damage cost distribution function $CDF_{UWM,p}(R_o)$ for a uniform population distribution (Eqn.14). In Fig.11, Eqns.13 and 14 are plotted in dimensionless form. Similar equations can be derived for secondary pollutants starting with Eqn.10b.

$$D_{UWM,p}(r) = Pop(r) C_p(r) \sum_i [S_{CR,i} U_{cost,i}] = \left[\frac{\Delta A}{2 \pi r} \frac{k_p}{u h_{mix}} e^{-\frac{k_p r}{u h_{mix}}} \right] D_{UWM,p} \quad (13)$$

$Pop(r)$ is the exposed population over the surface area ΔA at location r ($Pop(r) = \rho_{eff} \times \Delta A$). For an annular region $\frac{\Delta A}{2\pi r} = \Delta R$, the annulus thickness.

$$CDF_{UWM,p}(R_o) = Pop(R_o) \bar{C}_p(R_o) \sum_i [S_{CR,i} U_{cost,i}] = \left[1 - e^{-\frac{k_p R_o}{u h_{mix}}} \right] D_{UWM,p} \quad (14)$$

$Pop(R_o)$ is the number of people integrated over the interval $r \in [0, R_o]$ ($Pop(R_o) = \rho_{eff} \times \pi R_o^2$). Eqn.14 is simply the integral of Eqn.13 over the range $r = 0$ to $r = R_o$, with ΔA replaced by $2 \pi r dr$.

The exponential term in Eqn.14 is the regional share of the total impact ($r > R_o$). Eqn.15 is an improvement over Eqn.14 assuming different, but still uniformly distributed, local (ρ_{loc}) and background (ρ_{back}) receptor densities. R_{loc} is the local domain radius. The expression in the denominator is an ‘‘improved’’ estimate of the total impact assessment in which local and regional contributions are weighted according to their respective receptor densities. The ratio $\left(\frac{\rho_{loc}}{\rho_{back}} \right)$ varies

from 0.5 to 2 for typical European rural sites, whereas, for very large cities, such as London and Paris, the ratio can be as large as 15 ($R_{loc} = 56$ km). For typical European urban areas, the ratio lies between 6 and 10 (Tab.1). Eqn.15 is plotted in Fig.12 for various local-to-background density ratios. Profiles are similar to those presented in Fig.4. For $R_o < R_{loc}$, Eqn.14 is used with ρ_{eff} replaced by ρ_{loc} .

$$\left. \frac{CDF_{UWM,p}(R_o)}{D_{UWM,p}} \right|_{Improved} = 1 - \frac{\rho_{back} e^{-\lambda_p R_o}}{[\rho_{loc} (1 - e^{-\lambda_p R_{loc}}) + \rho_{back} e^{-\lambda_p R_{loc}}]} \quad (R_o > R_{loc}) \quad (15)$$

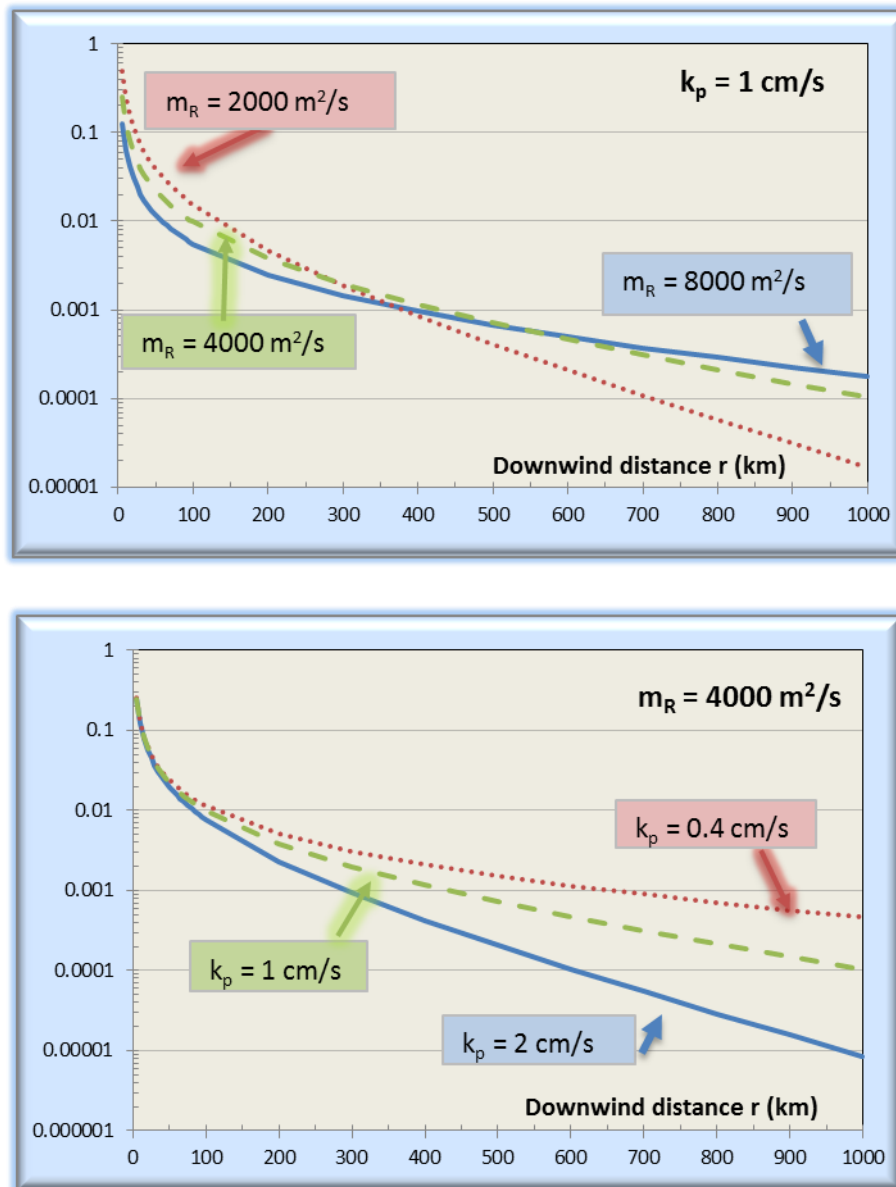


Fig.8. Influence of dilution and pollutant removal rates on the incremental downwind concentrations for a primary pollutant with an emission rate of 1 kt per year (Eqn.10a).

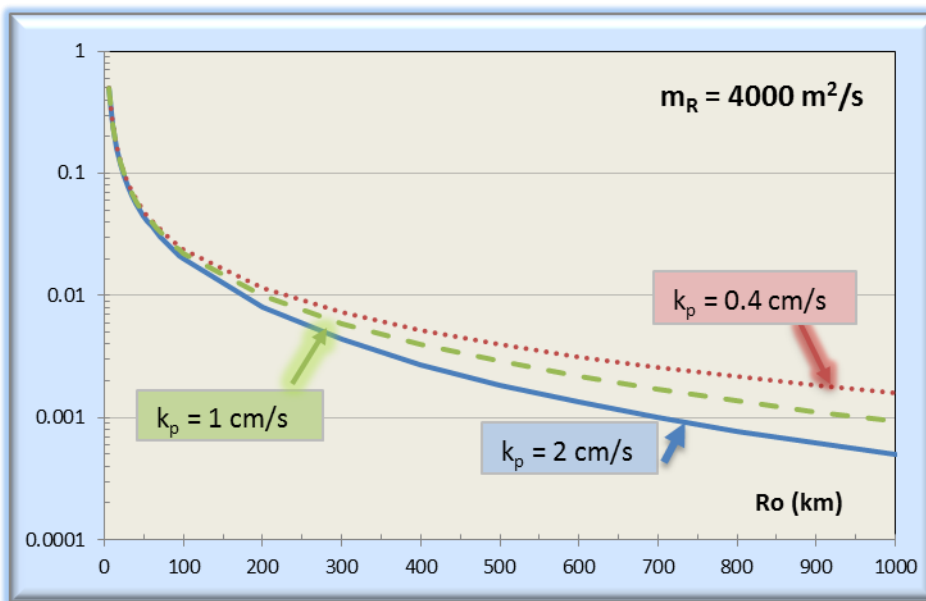
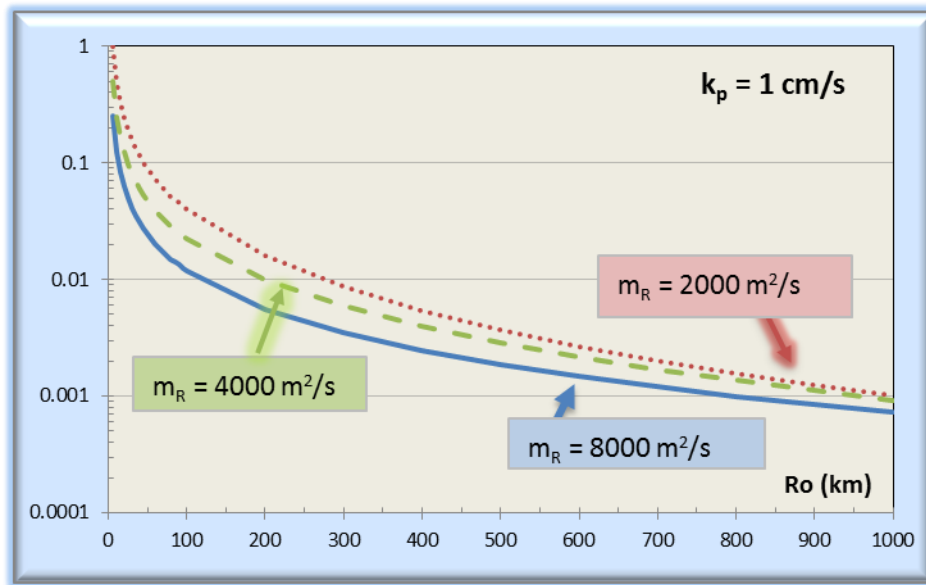


Fig.9. Influence of dilution and pollutant removal rates on the mean incremental concentration (averaged between 0 and R_o km) for a primary pollutant emission rate of 1 kt per year (Eqn.11).

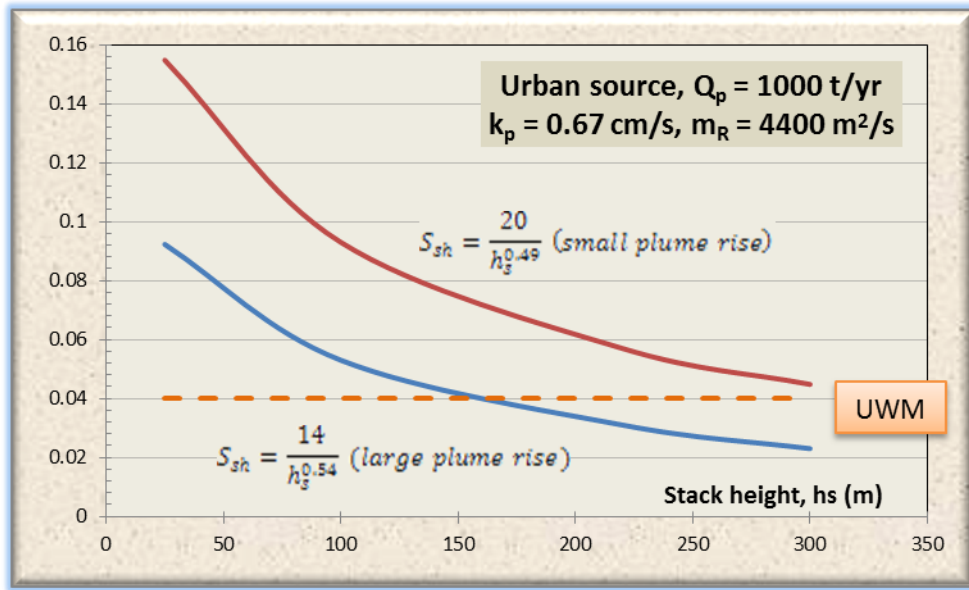


Fig.10. Comparison of UWM (Eqn.11) and ISC (EPA 1995) mean concentrations for a source located near Paris, France. Concentrations have been averaged over the range 0 to 56 km (R_0). Multiplier S_{sh} captures the influence of release height and is used to modify UWM estimates.

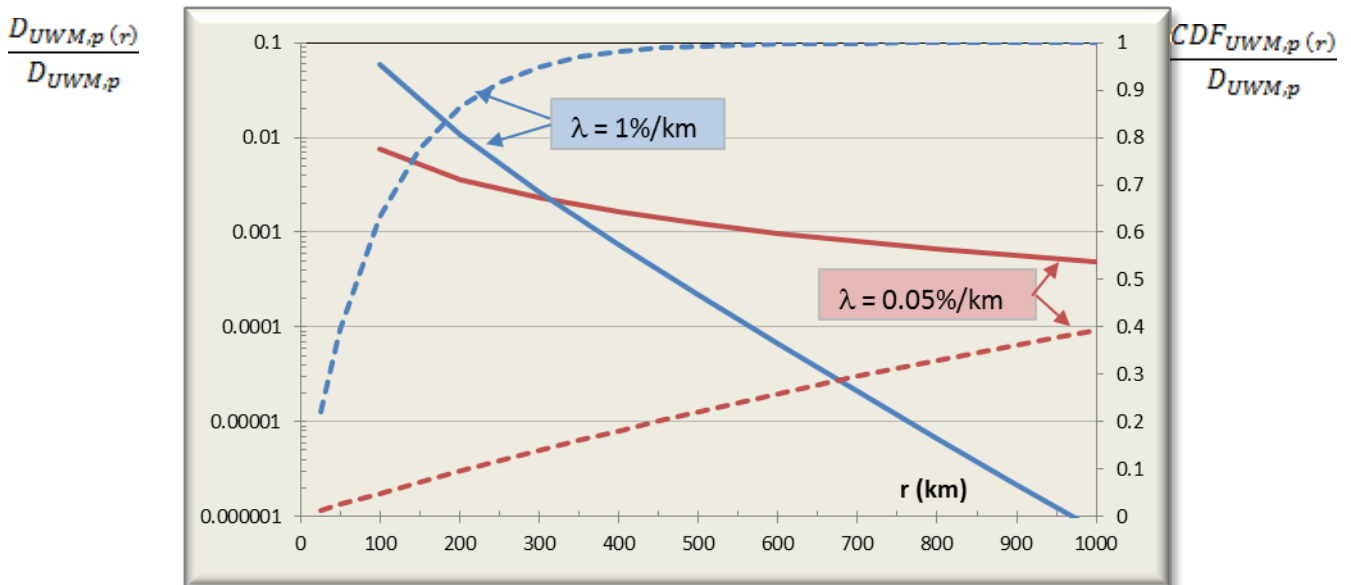


Fig.11. Normalized Uniform World Model damage cost (solid lines, left axis; Eqn.13) and cumulative damage distribution (dashed lines, right axis; Eqn.14) as a function of downwind distance from an elevated source for different pollutant decay constants (λ) and uniform population. $\Delta A = 10,000 \text{ km}^2$.

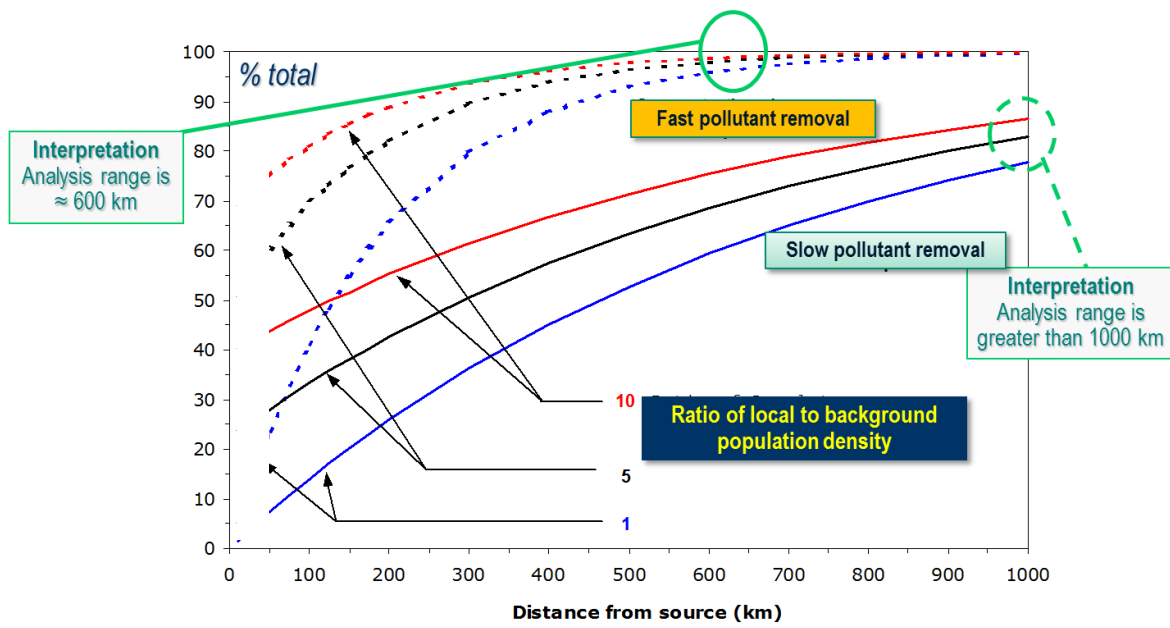


Fig.12. Plot of improved cumulative impact (damage cost) distribution function for various local-to-regional population densities and $R_{loc}=56$ km (Eqn.15). Results are consistent with profiles presented earlier in Fig.4.

4. Uniform World Model Comparisons

4.1. PM_{2.5} Marginal Damage Costs for Europe

Objective: Compute country-specific primary particulate matter (PPM) marginal damage costs (€/kg) using the UWM methodology (Eqn.8b) and compare with results from the NEEDS project of the European Commission (<http://www.needs-project.org/>). The objective of the NEEDS program is to evaluate the cost and benefits of different energy policies and future energy systems. The project is an interdisciplinary research program that brings together different fields of research.

Input data: Country-specific input information (ρ_{eff} and k_p), CRFs and unit costs are summarized in Tab.2 below. For the purpose of this exercise, particulate matter with aerodynamic size less than 2.5 μm was considered. ρ_{eff} is the effective receptor density, computed according to Eqn.5 ($f_{\text{loc}} = 15\%$), for a circular domain area characterized by a 1000 km radius and centered in the middle of the country of interest. ρ_{loc} , in most cases, was taken as the country-level population density.

Tab.2. UWM input data for PM_{2.5} marginal damage costs for Europe

Country	Population (millions of pers)	ρ_{EFF} pers/km ²	$k_{\text{PM2.5}}$ cm/s	Health Endpoint	PM _{2.5} CRF	U _{cost} [€/case]
Austria	8.3	110	0.56	Chronic mortality	6.51E-04	40000
Balkans	23.6	73	0.49	Infant Mortality	6.84E-08	3000000
Belgium	10.6	214	0.66	Chronic Bronchitis (new cases)	1.86E-05	200000
Bulgaria	7.6	53	0.49	Minor Restricted Activity days	3.69E-02	38
Cyprus	1.0	56	0.43	Net Restricted Activity days	9.59E-03	130
Czech Repl.	10.3	116	0.59	Work Days Lost	1.39E-02	295
Denmark	5.5	83	0.86	Hospital Admissions		
Estonia	1.3	33	0.62	Respiratory	7.03E-06	2000
Finland	5.3	36	0.62	Cardiac	4.34E-06	2000
France	61.7	105	0.45	Days Lower Respiratory Symptoms		
Germany	82.2	152	0.52	Adults	3.24E-02	38
Greece	11.2	55	0.49	Children	2.08E-02	38
Hungary	10.0	106	0.57	Bronchodilator		
Ireland	4.3	59	0.59	Adults	3.27E-03	1
Italy	59.1	150	0.71	Children	4.03E-04	1
Latvia	2.3	40	0.62			
Lithuania	3.4	52	0.62			
Luxembourg	0.5	138	0.59			
Malta	0.4	33	0.45			
Netherlands	16.4	228	0.66			
Norway	4.7	43	0.89			
Poland	38.1	97	0.57			
Portugal	10.6	62	0.54			
Romania	21.5	73	0.57			
Slovakia	5.4	106	0.58			
Slovenia	2.0	110	0.57			
Spain	45.3	55	0.50			
Sweden	9.1	75	0.86			
Switzerland	7.6	139	0.55			
UK	60.9	122	0.59			
Population weighted mean		113	0.57			

■ CRF in units of Annual cases per person per ug/m³

Results: UWM estimates are compared with NEEDS results in Fig.13. As can be seen, the maximum deviation at the country-level is only 26%. The mean deviation or “bias” is -0.4, UWM underestimates NEEDS predictions by less than 2% (mean relative error). The standard error and coefficient of variability are 2.2 and 0.1. At the continental-level, the UWM estimate is 25.7 €/kg of PM_{2.5}, which is just 5% higher than NEEDS. For PM₁₀, multiply PM_{2.5} results by 0.6, ratio of CRFs.

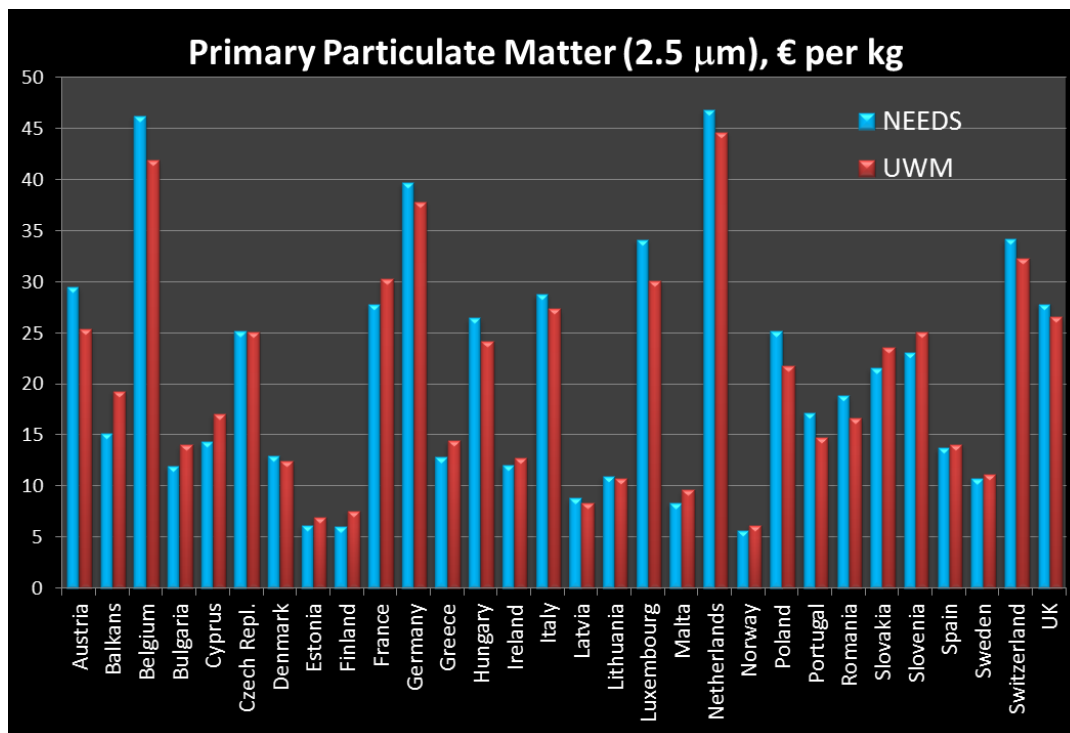
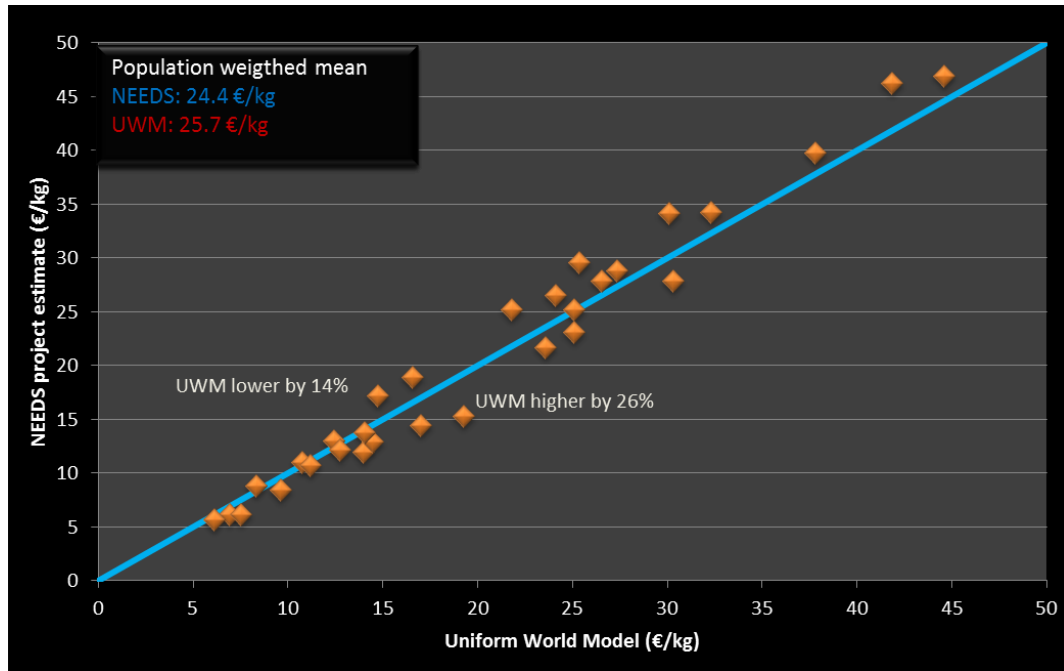


Fig.13. Primary particulates (PPM_{2.5}) marginal European damage costs: UWM vs. NEEDS.

4.2. Ammonia Marginal Damage Costs for Europe

Objective: Use the UWM methodology (Eqn.8b) for assessing the indirect health damage costs from ammonia emissions in Europe and compare with results from the EC4MACS project (<http://www.ec4macs.eu/home/index.html?sb=1>). The EC4MACS project is funded by the EU-LIFE program. Its main objective is to bring together international institutes renowned for their expertise and modeling capabilities in energy planning, environmental sciences (pollution transport and health and ecosystem impact assessment) and economics of pollution cost control strategies with the scope of assessing the cost-effectiveness of policies aimed at improving air quality in Europe and controlling emissions of greenhouse gases.

Input data: Tab.3 summarizes the UWM input data. The indirect consequences of ammonia emissions are quantified in terms of exposure to fine secondary particulate matter (SPM, PM_{2.5}), consisting of a mixture of ammonium sulfate and nitrate aerosols.

Tab.3. UWM input data for assessing ammonia marginal damage costs for Europe.

Country	P_{EFF} pers/km ²	k_{NH3} cm/s	Health Endpoint	PM _{2.5} CRF	U_{cost} [€/case]
Austria	110	1.05	Chronic mortality	6.51E-04	40000
Balkans	73	0.91	Infant Mortality	1.05E-07	1700000
Belgium	214	1.24	Chronic Bronchitis (new cases)	2.85E-05	208000
Bulgaria	53	0.91	Work Days Lost	6.06E-02	97
Czech Repl.	116	1.11	Hospital Admissions		
Denmark	83	1.61	Respiratory	1.08E-05	2364
Estonia	33	1.16	Cardiac	6.68E-06	2364
Finland	36	1.16	Days Lower Respiratory Symptoms		
France	105	0.84	Adults	4.91E-02	42
Germany	152	0.98	Children	3.19E-02	42
Greece	55	0.91	Bronchodilator		
Hungary	106	1.06	Adults	5.14E-03	1
Ireland	59	1.11	Children	6.21E-04	1
Italy	150	1.33			
Latvia	40	1.16			
Lithuania	52	1.16			
Luxembourg	138	1.11			
Malta	33	0.84			
Netherlands	228	1.24			
Norway	43	1.68			
Poland	97	1.08			
Portugal	62	1.01			
Romania	73	1.06			
Slovakia	106	1.09			
Slovenia	110	1.06			
Spain	55	0.94			
Sweden	75	1.61			
Switzerland	139	1.04			
UK	122	1.11			
Population weighted mean	113	1.07			

■ CRF in units of Annual cases per person per ug/m³

Results: UWM damage costs are compared with EC4MACS values in Fig.14. For most countries, deviations are within $\pm 30\%$, but the residuals scatter is greater, compared to primary $PM_{2.5}$ emissions, with standard deviation 3.4 and mean relative error is 5%. The larger scatter reflects the geographical variability in the chemical transformation rate, and consequently, the sulfates-to-nitrates mixture ratio. UWM estimates could be tweaked, according to the rules in Tab.1, if this ratio was known. At the pan-European level, the UWM overestimates EC4MACS by only 7.5%, remarkable given the complexities of chemical transformation (and uncertainties) involved.

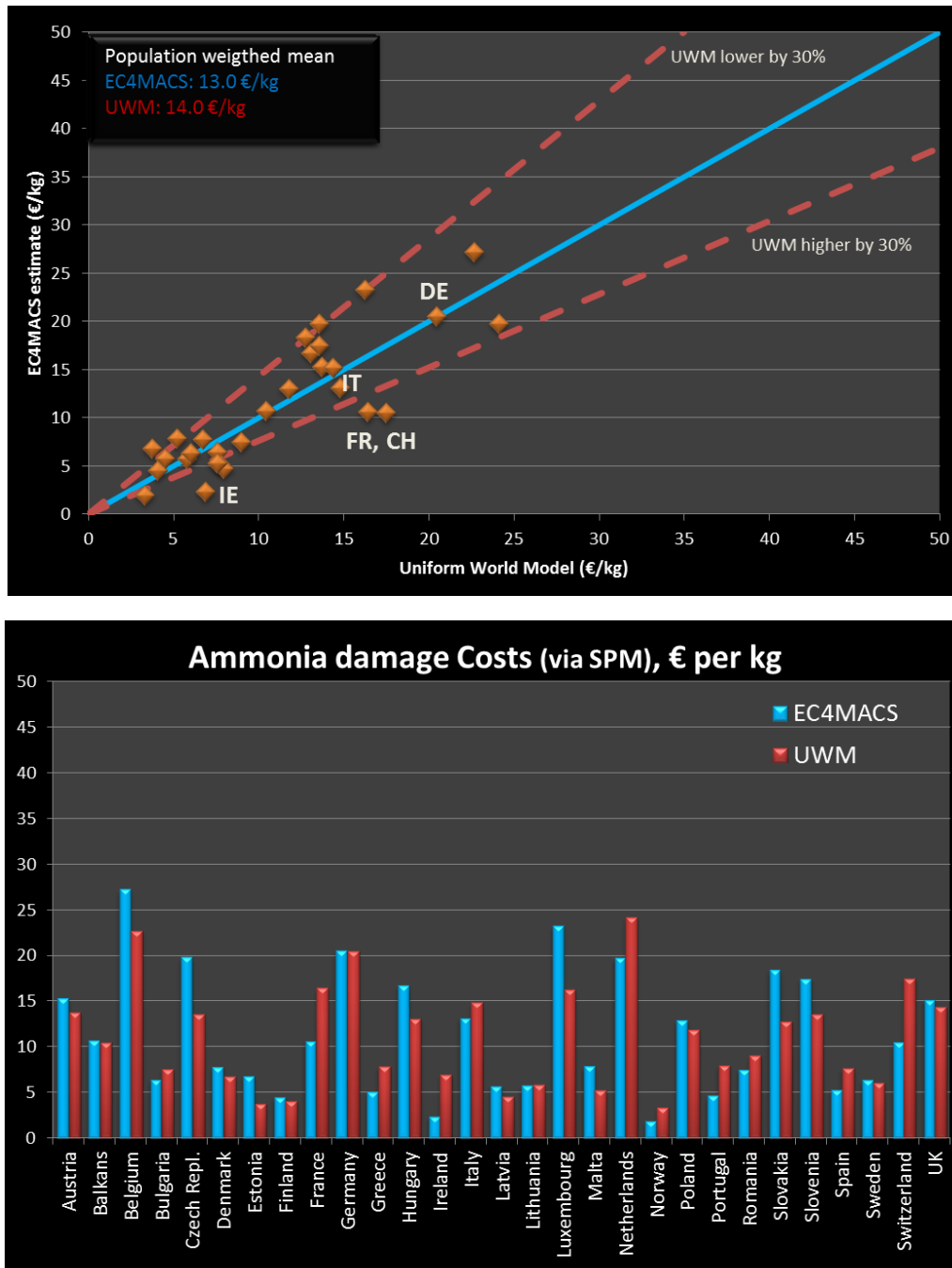


Fig.14. Marginal damage costs of ammonia emissions in Europe: UWM vs. EC4MACS (indirect impacts from formation of secondary particulate matter, SPM). IE = Ireland, FR = France, CH = Switzerland, IT = Italy and DE = Germany.

4.3. Air Pollution and Loss of Life Expectancy in China

Objective: Using the mean uniform world model incremental concentration (Eqn.6) estimate the loss of life expectancy (LLE) attributable to air pollutant emissions in China and compare the UWM estimate with the calculation performed with GAINS-China in Amann et al., (2008). GAINS is an integrated economic and environmental impact assessment model whose primary goal is to determine costs and benefits of multi-pollutant mitigation strategies for improving air quality, reducing deposition levels to aquatic and terrestrial environments and achieving specified climate targets (<http://gains.iiasa.ac.at/gains/EAS/index.login?logout=1>). The model brings together, in a consistent framework, information on atmospheric pollutant emissions, transformation and long-range dispersion, quantification of health and ecosystem impacts and pollution control costs. GAINS assesses emissions of greenhouse gas (CO₂, N₂O, CH₄ and f-gases), particulate matter, SO₂, NO_x, NH₃, volatile organic compounds (VOC) and tropospheric ozone (O₃).

Input data and Results: UWM input data and results, along with GAINS-China values for comparison, are summarized below in Tab.4. Details of the calculations are commented in the table footnote. The reduction in life expectancy (LE) from a lifetime exposure to a constant emission rate and mortality risk is computed using Eqn.16:

$$LLE = \bar{C}_{UWM} S_{CR} LE = \frac{Q_p S_{CR} LE}{A \times k} \quad (16)$$

where S_{CR} is the chronic mortality CRF (6.51E-4 YOLLs per [yr-pers- $\mu\text{g PM}_{2.5}/\text{m}^3$]), YOLL stands for years of life lost (LLE), LE is the Chinese population expected lifetime at birth (74 years) and A is the domain area (3.1 million km²), which in this case consists of the following regions: South-central, South-west and East China (Fig.15).

The agreement between UWM and GAINS-China models, as indicated in Tab.4, is quite good, the UWM underestimated by about 5%. The low and high UWM estimates represent the 68% confidence interval CI (or 1 standard deviation) about the mean estimate μ (Eqn.17). A geometric standard deviation σ_g of 1.5 has been assumed (Spadaro and Rabl, 2008). It is also worth pointing out that the mean UWM concentration (65 $\mu\text{g}/\text{m}^3$) is consistent with the concentration results shown in Fig.15.

$$68\% \text{ CI} = \mu e^{-0.5 \text{Ln}^2(\sigma_g)} \times \left[\frac{1}{\sigma_g}, \sigma_g \right] \quad (17)$$

In this analysis, the pollutant emission rates and mortality risks are assumed to remain constant over an individual's lifetime; both assumptions, of course, are not likely to be true half a century from now. Changes in emission rates and S_{CR} will depend on a number of variables linked to economic growth and technological, medical and political developments, including changes in fuel mix, pollution amount and toxicity, health risks (exposure and cause-specific cohort mortality rates), and so forth.

Tab.4. Loss of life expectancy (LLE) in China from anthropogenic emissions in 2005

Pollutant	Anthropogenic Emission kt/yr	k cm/s	\bar{C}_{UWM} $\mu\text{g}/\text{m}^3$	LLE (in months)					
				UWM			GAINS-China		
				mean	low	high	mean	low	high
PM _{2.5}	12,725	0.62	21.3	12.3	7.0	15.7			
SO ₂	31,528	1.96	16.7	9.6	5.4	12.3			
NO _x	16,926	0.88	9.9	5.7	3.2	7.3			
NH ₃	12,844	0.77	17.2	10.0	5.6	12.7			
ALL			65.1	37.7	21.3	47.9	39.4	20.6	53.1

Footnotes

- Anthropogenic emissions data from Tab 2.3 in Amann et al., 2008 (p.10)
- Mean UWM incremental concentration from Eqn.6 (domain area 3.066 million km², and includes South-central, South-east & East China; area roughly corresponds to a circular region of radius 1000 km that is centered in the Province of Hubei)
- For NO_x emissions, a correction factor $S_{ct} = 0.5$ (Tab.1) has been applied in computing mean concentration of inorganic nitrate aerosols
- UWM LLE estimate from Eqn.16 (long-term mortality CRF 6.51E-4 Annual LLE per [pers- μg PM_{2.5}/m³]; life expectancy at birth 74 years)
- Low and high UWM estimates correspond to 68% confidence interval (Eqn.17)
- GAINS-China LLE estimates from Tab 2.5 in Amann et al., 2008 (p.16)

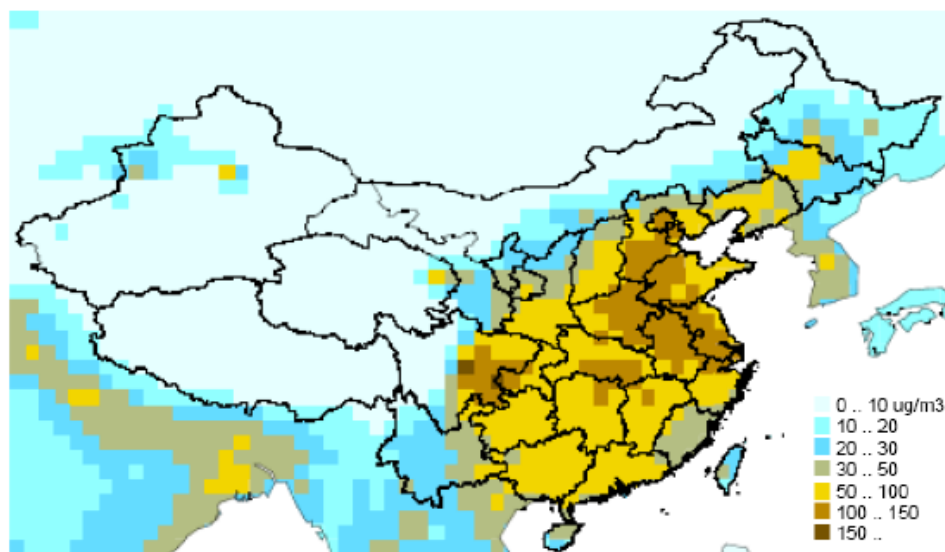


Fig.15. Fine particulate matter (PM_{2.5}) ambient concentrations for anthropogenic emissions in China, 2005. Particulate concentrations include primary emissions and secondary inorganic aerosols formed from primary releases of NO_x, SO₂ and NH₃. (Ref: Amann et al., 2008)

4.4. Source-Receptor Relationships (SRR) for Europe

Objective:The aim in this section is to compute incremental concentrations at the country- and continental-level (receptor or receiving area) due to primary pollutant emissions of PM, SO₂, NO_x and ammonia for select countries in Europe (emitter or source country). UWM (Eqns. 6 and 11) predictions are compared with results from source-receptor relationships (SSR), also known as country-to-country “blame matrices” provided by the European Monitoring and Evaluation Programme (EMEP) model. An example of a SSR is given in Tab.5 for primary PM_{2.5} (PPM_{2.5}) emissions in 2004. Each column indicates an emitter country and each row is the receptor country. The values listed in the table represent the (anticipated) PPM_{2.5} background concentration change in a given country (ng/m³) resulting from a 15% emission reduction in another country. Moving down a column identifies where a pollutant ends up once it is emitted into the air from a specified country (fate analysis), and across a row the contribution to the change in air quality in that country due to emissions transported from another country or due to its own emissions.

The EMEP model (<http://www.emep.int/>) is part of the core models used in the EC4MACS program, and has been used extensively in support of policymaking decisions under the Convention on Long-Range Transboundary Air Pollution (CLRTAP, <http://www.unece.org/env/lrtap/welcome.html>). The model has been developed by the *Meteorological Synthesizing Centre-West*, which is hosted by the Norwegian Meteorological Institute in Oslo, Norway (MET.NO) since the inception of the EMEP programme in 1979. The EMEP model is a multi-layer atmospheric dispersion model for simulating the long-range transport of air pollution, including estimation of spatial concentration patterns and deposition fluxes that contribute to acidification and eutrophication of terrestrial and aquatic environments. EMEP models the transport of atmospheric particles, both fine (<2.5µm) and coarse shares (between 2.5 and 10 µm), SO₂, NO_x, non-methane volatile organic species (NMVOC), heavy metals (HM), persistent organic pollutants (POP) and ground-level ozone (O₃). The range of the analysis covers the entire northern hemisphere, at a resolution of 150 by 150 km. At the European scale, the grid resolution has been refined to a size of 50 by 50 km.

Input data and results: Input values, UWM estimates and comparisons with EMEP results are shown in Tabs. 6 and 7, and in graphical format in Figs.16 and 17. Comparisons at the European continental level are summarized in Tab.6, whereas country-specific air quality changes due to own emissions, are provided in Tab.7. Table footnotes provide additional computation details. For the case of continental changes, on average, the UWM overestimates PPM_{2.5} concentrations by 2.5% and for secondary PM by 10.2%. With the exception of two cases, the minimum and maximum deviations are -25% and +39%. At the country-level, the UWM, on average, underestimates PPM_{2.5} concentrations by about 5%, with the largest differences (±30%) noted for countries bordering Europe (UK and Finland, for example).

Tab.5. 2004 EMEP source receptor relationships (“blame matrices”) for primary PM_{2.5}, change in mean background concentration (ng/m³) in receiver (receptor) country (table row) for a 15% emission reduction in source (emitter) country (table column).

	AL	AM	AT	AZ	BA	BE	BG	BY	CH	CS	CY	CZ	DE	DK	EE	ES	FI	FR	GB	GE	GR	HR	HU	IE	IS	IT	KZ	LT	
AL	22	0	1	0	2	0	6	0	0	23	0	1	1	0	0	1	0	2	0	0	45	1	2	0	12	0	0	AL	
AM	0	0	0	4	0	0	0	0	0	0	0	0	0	0	0	0	0	0	0	0	0	0	0	0	0	0	0	AM	
AT	0	0	76	0	0	1	0	0	1	2	0	14	13	0	0	1	0	11	1	0	0	4	13	0	19	0	0	AT	
AZ	0	0	0	15	0	0	0	0	0	0	0	0	0	0	0	0	0	0	1	0	0	0	0	0	0	1	0	AZ	
BA	0	0	3	0	38	0	2	0	0	35	0	3	2	0	0	1	0	4	0	0	1	11	7	0	15	0	0	BA	
BE	0	0	1	0	0	160	0	0	0	0	0	2	76	1	0	2	0	110	15	0	0	0	0	0	1	0	0	BE	
BG	0	0	1	0	1	0	88	1	0	9	0	1	1	0	0	0	2	0	0	11	1	3	0	4	0	0	0	BG	
BY	0	0	0	0	0	0	1	72	0	1	0	1	2	0	2	0	1	2	0	0	0	2	0	1	0	5	0	BY	
CH	0	0	7	0	0	1	0	0	34	0	0	0	11	0	0	1	0	26	1	0	0	0	0	0	37	0	0	CH	
CS	3	0	2	0	6	0	14	0	0	83	0	2	2	0	0	1	0	3	0	0	4	3	10	0	10	0	0	CS	
CY	0	0	0	0	0	2	0	0	0	6	0	0	0	0	0	0	0	0	0	3	0	0	0	0	1	0	0	CY	
CZ	0	0	17	0	0	1	0	0	1	2	0	106	23	1	0	1	0	15	1	0	0	1	7	0	5	0	0	CZ	
DE	0	0	9	0	0	6	0	0	3	0	0	14	104	3	0	1	0	34	5	0	0	1	0	4	0	0	0	DE	
DK	0	0	0	0	0	2	0	0	0	0	0	2	14	67	0	0	1	8	7	0	0	0	0	0	0	0	0	DK	
EE	0	0	0	0	0	0	0	5	0	0	0	1	2	1	65	0	14	1	1	0	0	0	0	0	0	0	5	EE	
ES	0	0	0	0	0	0	0	0	0	0	0	1	0	0	96	0	25	1	0	0	0	0	0	2	0	0	0	ES	
FI	0	0	0	0	0	0	0	1	0	0	0	0	0	0	8	0	52	0	0	0	0	0	0	0	0	0	1	FI	
FR	0	0	0	0	0	10	0	0	3	0	0	0	12	0	0	9	0	229	6	0	0	0	0	0	10	0	0	FR	
GB	0	0	0	0	0	4	0	0	0	0	0	0	4	0	0	0	0	21	90	0	0	0	0	2	0	0	0	GB	
GE	0	0	0	4	0	0	0	0	0	0	0	0	0	0	0	0	0	0	0	12	0	0	0	0	0	0	0	GE	
GL	0	0	0	0	0	0	0	0	0	0	0	0	0	0	0	0	0	0	0	0	0	0	0	0	0	0	0	GL	
GR	1	0	0	0	1	0	18	0	0	6	0	0	1	0	0	1	0	2	0	0	69	0	1	0	7	0	0	GR	
HR	0	0	8	0	16	0	2	0	0	23	0	5	4	0	0	1	0	7	0	0	1	49	16	0	24	0	0	HR	
HU	0	0	8	0	3	0	2	1	0	18	0	8	6	0	0	0	7	0	0	0	8	86	0	10	0	0	0	HU	
IE	0	0	0	0	0	0	0	0	0	0	0	0	1	0	0	0	0	9	17	0	0	0	25	0	0	0	0	IE	
IS	0	0	0	0	0	0	0	0	0	0	0	0	0	0	0	0	0	0	1	0	0	0	0	0	0	0	0	IS	
IT	0	0	4	0	2	0	1	0	1	2	0	1	2	0	0	4	0	15	0	0	1	4	1	0	149	0	0	IT	
KZ	0	0	0	0	0	0	0	0	0	0	0	0	0	0	0	0	0	0	0	0	0	0	0	0	13	0	0	KZ	
LT	0	0	0	0	0	0	0	26	0	0	0	2	3	2	4	0	3	3	1	0	0	0	1	0	1	0	64	LT	
LU	0	0	2	0	0	20	0	0	2	0	0	3	96	1	0	3	0	134	8	0	0	0	0	2	0	0	0	LU	
LV	0	0	0	0	0	0	0	20	0	0	0	1	3	2	12	0	5	2	1	0	0	0	0	0	0	20	0	LV	
MD	0	0	1	0	0	0	7	2	0	2	0	1	1	0	0	0	0	2	0	0	1	0	2	0	2	0	0	MD	
MK	4	0	1	0	2	0	23	0	0	18	0	1	1	0	0	1	0	2	0	0	40	1	2	0	8	0	0	MK	
MT	0	0	0	0	1	0	1	0	0	2	0	0	1	0	0	5	0	12	0	0	2	1	0	0	38	0	0	MT	
NL	0	0	1	0	0	35	0	0	0	0	0	2	97	3	0	1	0	48	17	0	0	0	0	1	0	0	0	NL	
NO	0	0	0	0	0	0	0	0	0	0	0	0	1	0	0	1	0	1	0	0	0	0	0	0	0	0	0	0	NO
PL	0	0	2	0	0	1	0	7	0	1	0	12	13	2	1	0	1	7	1	0	0	0	4	0	2	0	3	PL	
PT	0	0	0	0	0	0	0	0	0	0	0	0	0	0	0	50	0	9	0	0	0	0	0	0	0	0	0	0	PT
RO	0	0	1	0	1	0	16	1	0	8	0	2	2	0	0	0	0	3	0	0	2	1	6	0	4	0	0	RO	
RU	0	0	0	0	0	0	2	0	0	0	0	0	0	1	0	2	0	0	0	0	0	0	0	0	2	0	0	RU	
SE	0	0	0	0	0	0	1	0	0	0	0	2	3	2	0	8	1	1	0	0	0	0	0	0	0	1	0	SE	
SI	0	0	24	0	3	0	1	0	0	6	0	8	7	0	0	1	0	8	0	0	0	61	15	0	39	0	0	SI	
SK	0	0	6	0	1	0	1	1	0	6	0	14	7	0	0	0	0	7	0	0	0	2	42	0	6	0	0	SK	
TR	0	0	0	0	0	0	2	0	0	0	0	0	0	0	0	0	0	0	0	1	0	0	0	0	0	0	0	TR	
UA	0	0	0	0	0	0	3	5	0	1	0	1	1	0	0	0	1	0	0	0	0	2	0	1	0	0	0	UA	
ATL	0	0	0	0	0	0	0	0	0	0	0	0	0	0	0	1	0	4	1	0	0	0	0	0	0	0	0	ATL	
BAS	0	0	0	0	0	1	0	2	0	0	0	1	7	10	11	0	20	4	2	0	0	0	0	0	0	4	0	BAS	
BLS	0	0	0	0	0	0	5	1	0	1	0	0	0	0	0	0	1	0	0	2	0	0	0	1	0	0	0	BLS	
MED	1	0	1	0	1	0	3	0	0	2	0	0	1	0	0	8	0	16	0	0	8	1	0	0	24	0	0	MED	
NOS	0	0	0	0	0	5	0	0	0	0	0	0	9	5	0	0	0	24	22	0	0	0	1	0	0	0	0	NOS	
ASI	0	0	0	0	0	0	0	0	0	0	0	0	0	0	0	0	0	0	0	0	0	0	0	0	1	0	0	ASI	
NOA	0	0	0	0	0	0	1	0	0	1	0	0	0	0	0	3	0	4	0	0	2	0	0	0	5	0	0	NOA	
EMC	0	0	1	0	0	1	1	2	0	1	0	1	4	0	0	4	2	12	2	0	1	0	1	0	5	1	0	EMC	
EU	0	0	4	0	0	4	0	1	0	1	0	5	16	2	2	15	5	44	8	0	2	1	3	0	15	0	2	EU	

Concentration change in Germany due to 15% reduction in German emissions

Concentration change at the EU-level from a 15% emission decrease in the country at the top of the column.

Tab.5 (cont.) 2004 EMEP source receptor relationships (“blame matrices”) for primary PM_{2.5}, change in mean background concentration (ng/m³) in receiver (receptor) country (table row) for a 15% emission reduction in source (emitter) country (table column).

	LU	LV	MD	MK	MT	NL	NO	PL	PT	RO	RU	SE	SI	SK	TR	UA	ATL	BAS	BLS	MED	NOS	ASI	NOA	BIC	DMS	VOL	EU		
AL	0	0	0	18	0	0	0	2	0	4	1	0	0	1	1	2	0	0	0	7	0	0	0	0	0	0	74	AL	
AM	0	0	0	0	0	0	0	0	0	0	3	0	0	0	36	1	0	0	0	0	0	7	0	0	0	0	1	AM	
AT	0	0	0	0	0	0	0	9	0	2	0	0	8	18	0	1	0	0	0	1	1	0	0	0	0	0	192	AT	
AZ	0	0	0	0	0	0	0	0	0	0	13	0	0	0	15	2	0	0	0	0	0	17	0	0	0	0	1	AZ	
BA	0	0	0	0	0	0	0	7	0	4	0	0	1	4	0	1	0	0	0	4	0	0	0	0	0	0	56	BA	
BE	7	0	0	0	0	50	1	2	1	0	0	1	0	0	0	1	0	0	0	22	0	0	0	0	0	0	438	BE	
BG	0	0	3	1	0	0	0	4	0	36	7	0	0	2	21	16	0	0	4	3	0	0	0	0	0	0	36	BG	
BY	0	3	2	0	0	0	0	17	0	5	34	1	0	3	0	44	0	1	0	0	0	0	0	0	0	0	49	BY	
CH	0	0	0	0	0	0	0	1	0	0	0	0	0	0	0	0	0	0	0	1	1	0	0	0	0	0	92	CH	
CS	0	0	0	4	0	0	0	6	0	22	1	0	0	5	1	4	0	0	0	3	0	0	0	0	0	0	54	CS	
CY	0	0	0	0	0	0	0	0	0	2	3	0	0	0	68	4	0	0	0	22	0	3	0	0	0	0	14	CY	
CZ	0	0	0	0	0	1	0	46	0	2	1	1	1	25	0	2	0	1	0	0	1	0	0	0	0	0	261	CZ	
DE	0	0	0	0	0	6	1	13	0	0	1	2	0	1	0	0	0	4	0	0	7	0	0	0	0	0	211	DE	
DK	0	0	0	0	0	2	10	13	0	0	4	19	0	1	0	1	0	41	0	0	16	0	0	0	0	0	146	DK	
EE	0	14	0	0	0	0	3	7	0	0	48	8	0	0	0	5	0	7	0	0	1	0	0	0	0	0	127	EE	
ES	0	0	0	0	0	0	0	0	11	0	0	0	0	0	0	0	2	0	0	10	0	0	0	0	0	0	141	ES	
FI	0	1	0	0	0	0	3	2	0	0	24	7	0	0	0	2	0	3	0	0	0	0	0	0	0	0	77	FI	
FR	1	0	0	0	0	3	0	0	1	0	0	0	0	0	0	0	2	0	0	3	5	0	0	0	0	0	290	FR	
GB	0	0	0	0	0	3	1	1	0	0	0	0	0	0	0	0	4	0	0	0	21	0	0	0	0	0	133	GB	
GE	0	0	0	0	0	0	0	0	0	0	10	0	0	0	0	31	3	0	0	0	0	2	0	0	0	0	2	GE	
GL	0	0	0	0	0	0	0	0	0	0	0	0	0	0	0	0	0	0	0	0	0	0	0	0	0	0	0	GL	
GR	0	0	1	3	0	0	0	2	0	9	4	0	0	1	21	8	0	0	0	19	0	0	0	0	0	0	0	90	GR
HR	0	0	0	0	0	0	0	10	0	5	1	0	4	7	0	2	0	0	0	5	0	0	0	0	0	0	0	95	HR
HU	0	0	0	0	0	0	0	22	0	31	2	0	2	29	0	11	0	0	0	1	0	0	0	0	0	0	0	189	HU
IE	0	0	0	0	0	0	0	0	0	0	0	0	0	0	0	0	9	0	0	0	2	0	0	0	0	0	58	IE	
IS	0	0	0	0	0	0	0	0	0	0	0	0	0	0	0	0	0	0	0	0	0	0	0	0	0	0	3	IS	
IT	0	0	0	0	0	0	0	2	0	1	0	0	3	1	1	0	0	0	0	20	0	0	0	0	0	0	0	193	IT
KZ	0	0	0	0	0	0	0	0	0	0	32	0	0	0	1	8	0	0	0	0	0	0	0	0	0	0	0	2	KZ
LT	0	14	0	0	0	0	0	2	24	0	2	19	4	0	2	0	11	0	3	0	1	0	0	0	0	0	0	137	LT
LU	14	0	0	0	0	9	1	2	0	0	0	0	0	0	0	0	1	0	0	0	7	0	0	0	0	0	0	302	LU
LV	0	48	0	0	0	0	2	13	0	1	25	6	0	1	0	8	0	5	0	0	1	0	0	0	0	0	0	122	LV
MD	0	0	125	0	0	0	0	9	0	38	15	0	0	2	8	88	0	0	2	0	0	0	0	0	0	0	0	29	MD
MK	0	0	0	22	0	0	0	2	0	7	2	0	0	1	4	4	0	0	0	4	0	0	0	0	0	0	0	65	MK
MT	0	0	0	0	3	0	0	1	0	1	0	0	0	0	1	1	0	0	0	91	0	0	1	0	0	0	0	70	MT
NL	0	0	0	0	0	92	2	3	1	0	1	1	0	0	0	0	1	1	0	0	32	0	0	0	0	0	0	311	NL
NO	0	0	0	0	0	0	37	1	0	0	3	5	0	0	0	1	0	1	0	0	2	0	0	0	0	0	0	15	NO
PL	0	1	0	0	0	1	1	144	0	3	7	2	0	10	0	17	0	3	0	0	2	0	0	0	0	0	0	217	PL
PT	0	0	0	0	0	0	0	0	115	0	0	0	0	0	0	0	7	0	0	2	0	0	0	0	0	0	0	179	PT
RO	0	0	16	0	0	0	0	9	0	147	7	0	0	4	6	25	0	0	2	1	0	0	0	0	0	0	0	41	RO
RU	0	0	0	0	0	0	0	1	0	1	128	1	0	0	2	12	0	0	0	0	0	0	0	0	0	0	0	10	RU
SE	0	1	0	0	0	0	11	5	0	0	6	34	0	0	0	2	0	6	0	0	2	0	0	0	0	0	0	64	SE
SI	0	0	0	0	0	0	0	9	0	3	1	0	50	6	0	2	0	0	0	5	0	0	0	0	0	0	0	177	SI
SK	0	0	0	0	0	0	0	49	0	11	2	0	1	91	0	18	0	0	0	0	0	0	0	0	0	0	0	235	SK
TR	0	0	0	0	0	0	0	0	0	2	5	0	0	0	125	6	0	0	0	3	0	2	0	0	0	0	0	6	TR
UA	0	0	8	0	0	0	0	11	0	13	42	0	0	2	8	208	0	0	1	0	0	0	0	0	0	0	0	30	UA
ATL	0	0	0	0	0	0	1	0	3	0	1	0	0	0	0	0	4	0	0	0	0	0	0	0	0	0	0	14	ATL
BAS	0	6	0	0	0	1	6	16	0	0	23	20	0	1	0	3	0	25	0	0	4	0	0	0	0	0	0	113	BAS
BLS	0	0	4	0	0	0	0	3	0	9	38	0	0	1	68	44	0	0	10	2	0	0	0	0	0	0	0	13	BLS
MED	0	0	0	0	0	0	0	1	1	2	1	0	0	0	20	3	0	0	0	57	0	1	1	0	0	0	0	67	MED
NOS	0	0	0	0	0	8	13	2	0	0	1	3	0	0	0	2	2	0	0	42	0	0	0	0	0	0	0	87	NOS
ASI	0	0	0	0	0	0	0	0	0	0	7	0	0	0	12	2	0	0	1	0	17	0	0	0	0	0	0	1	ASI
NOA	0	0	0	0	0	0	0	0	0	1	0	0	0	0	4	1	0	0	0	12	0	0	4	0	0	0	0	20	NOA
EMC	0	0	1	0	0	0	1	5	1	4	35	1	0	1	9	13	0	0	0	3	1	1	0	0	0	0	0	51	EMC
EU	0	1	0	0	0	2	2	17	4	1	5	5	0	4	1	3	1	2	0	4	4	0	0	0	0	0	0	171	EU

Tab.6. Influence of country emissions on the mean European incremental concentration

Emitter country		UWM				EMEP (SRR)	
Pollutant	Q _p for 2004 kt	k cm/s	A km ²	\bar{C}_{UWM} Eqn.6 ng/m ³	$\frac{\bar{C}_{UWM}}{Q_p}$ ng/m ³ per kt	$\Delta C_{15\%}$ ng/m ³	$\frac{\Delta C}{Q_p}$ ng/m ³ per kt
FRANCE							
PM _{2.5}	325	0.45	7.1E+06	324	1.00	44	0.90
SO ₂	484	1.73	9.6E+06	92	0.19	14	0.19
NOx	1,218	0.71	9.6E+06	565	0.23	36	0.20
NH ₃	742	0.56	9.6E+06	435	0.59	40	0.36
GERMANY							
PM _{2.5}	105	0.52	7.1E+06	91	0.86	16	1.02
SO ₂	559	1.94	9.6E+06	95	0.17	19	0.23
NOx	1,594	0.83	9.6E+06	633	0.20	47	0.20
NH ₃	641	0.65	9.6E+06	325	0.51	52	0.54
ITALY							
PM _{2.5}	161	0.71	7.1E+06	102	0.63	15	0.62
SO ₂	418	1.50	9.6E+06	92	0.22	10	0.16
NOx	1,244	0.85	9.6E+06	482	0.19	26	0.14
NH ₃	412	0.89	9.6E+06	153	0.37	19	0.31
POLAND							
PM _{2.5}	134	0.57	7.1E+06	105	0.79	17	0.85
SO ₂	1,286	1.98	9.6E+06	214	0.17	35	0.18
NOx	804	1.27	9.6E+06	209	0.13	17	0.14
NH ₃	317	0.71	9.6E+06	147	0.46	28	0.59
UK							
PM _{2.5}	96	0.59	7.1E+06	73	0.76	8	0.56
SO ₂	833	2.10	9.6E+06	131	0.16	17	0.14
NOx	1,621	1.20	9.6E+06	445	0.14	15	0.06
NH ₃	336	0.74	9.6E+06	150	0.45	19	0.38

Footnotes

- Precursor emission rates taken from EMEP database (http://www.emep.int/mscw/mscw_publications.html).
- Mean UWM incremental concentration from Eqn.6; SO₂, NOx and NH₃ results are for secondary inorganic aerosols.
- A is the averaging surface area, corresponding to a circle of radius 1,500 km for PM_{2.5} and 1,750 km for others.
- For NOx emissions, a correction factor S_{ct} = 0.5 (Tab.1) has been applied in the computation of nitrate aerosols.
- $\Delta C_{15\%}$ is the change in the European concentration (receptor) for a 15% pollutant reduction in the source country.
- According to Tab.5, for the case of Germany as an emitter, a 15% PPM_{2.5} reduction would result in a change of 104 ng/m³ in the background concentration across Germany (receptor). The UWM methodology (Eqn.11) can be used to compute this estimate. Assuming a value of 340 km for R_o (German equivalent size, if the country were a circle) and a dilution rate of 4000 m²/s, Eqn.11 predicts a mean PPM_{2.5} concentration of 640 ng/m³, across the whole of Germany. 15% of this value is 96 ng/m³, which is consistent with the EMEP prediction, deviation is less than 8%.

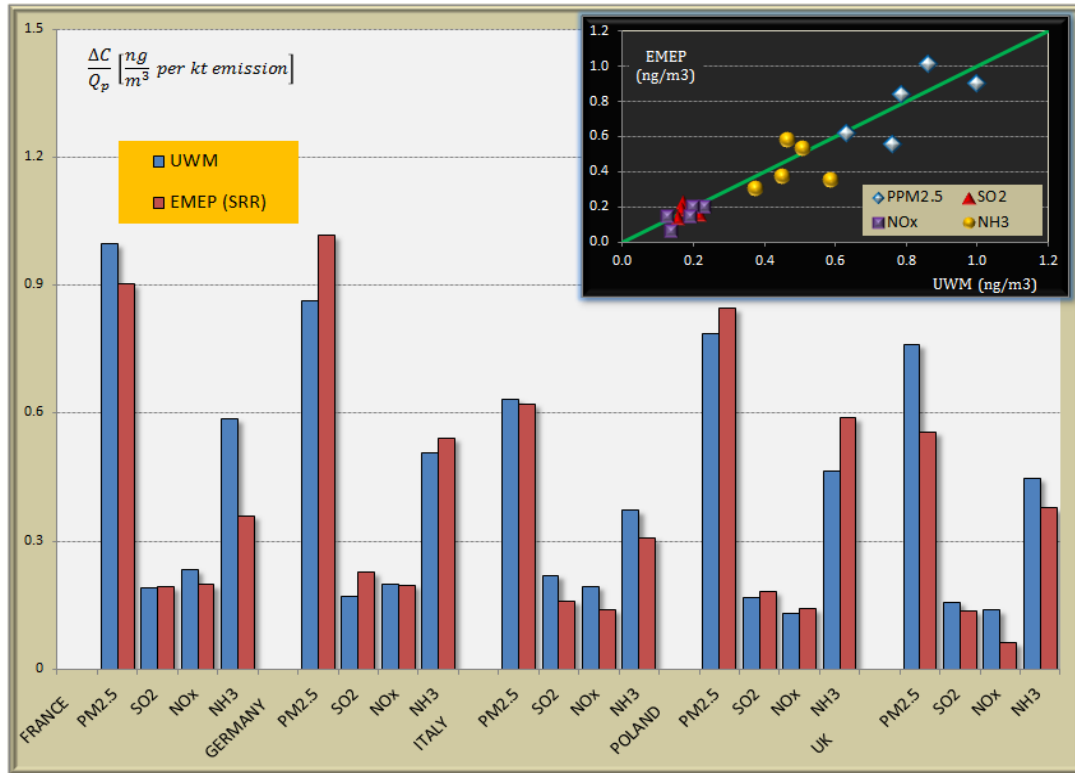


Fig.16. Contribution of country-level emissions to changes in the mean concentration at the pan-European scale, comparison of UWM and EMEP results (2004).

Tab.7. Country-level PPM_{2.5} mean concentration changes due to own country emissions, 2004

Emitter			UWM			$\Delta C_{15\%} (ng/m^3)$	
Country	Geographical area 1000's km ²	Q _p for 2004 kt	k cm/s	Ro km	$\bar{C}_p(R_o)$ Eqn.11 ng/m ³	UWM	EMEP
Germany	357	105	0.52	337	636	95	104
Czech Repl.	78.9	36	0.59	158	511	77	106
Finland	338	39	0.62	328	235	35	52
France	552	325	0.45	419	1560	234	229
Poland	313	134	0.57	316	863	129	144
Serbia	91.3	43	0.49	170	574	86	83
Spain	505	145	0.50	401	718	108	107
UK	244	105	0.52	279	798	120	90

Footnotes

- Precursor emission rates taken from EMEP database (http://www.emep.int/mscw/mscw_publications.html).
- Mean UWM incremental concentration calculated from Eqn.11 ($r = 0$ to R_o).
- R_o is the radius of a circular region of area πR_o^2 that is equal to the geographical area of the country in question.
- A dilution rate (ventilation index) equal to $4000 \text{ m}^2/\text{s}$ has been assumed for UWM computations.
- $\Delta C_{15\%}$ is the mean change in air concentration over the whole country for a 15% emission reduction in that country.

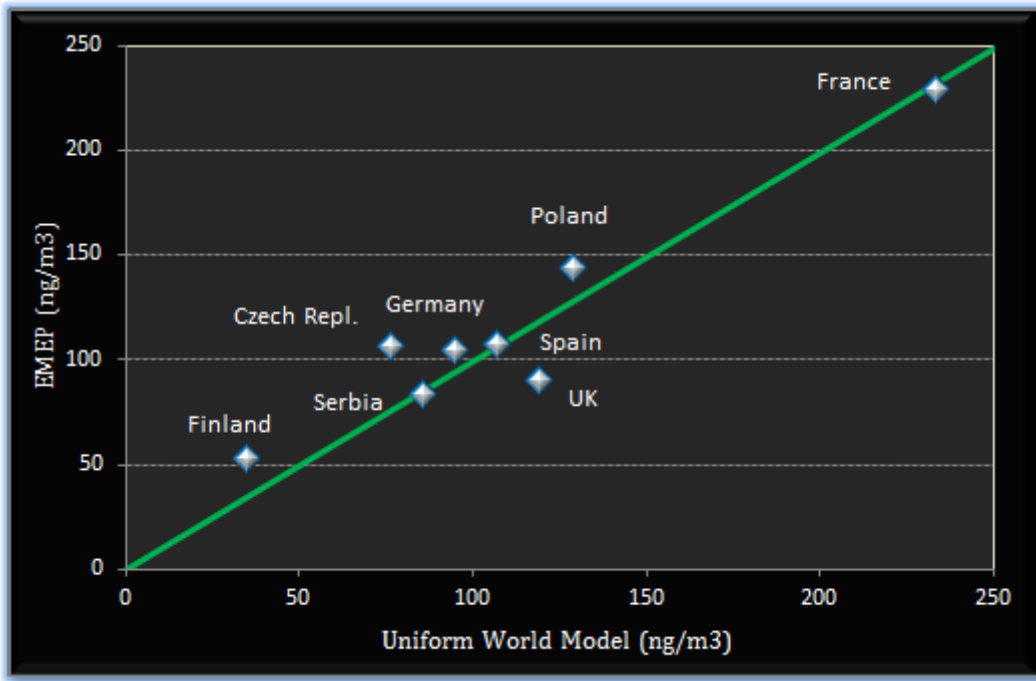


Fig.17. Comparison of UWM and EMEP country-level PPM_{2.5} concentration for emissions in 2004 (change in local air quality due to own emissions)

4.5. Intake factors for PM_{2.5} and Inorganic Secondary Particulate Matter

Objective: The goal is to compute the pollutant intake factor iF using the UWM methodology (Eqn.7) and then to compare with values reported in the literature for the United States and China. The relevant exposure pathway is inhalation.

Input data and results: Tab.8 summarizes the input data used in this analysis and iF comparisons with literature results. In the original studies, the concentration spatial profiles were estimated using the CALPUFF atmospheric long-range transport model (EPA 1998b), and for the intake dose a daily breathing rate of 20 m³ was assumed. The UWM uncertainty intervals were calculated assuming $\sigma_g=1.5$. Further computational details have been summarized in the table footnotes.

As seen from Tab.8, independent of the scale of the analysis – local, regional or national, comparisons are quite favorable for primary particulate emissions, with typical deviations less than 10% and a max difference of 26%. The UWM model tends to over-predict the exposure. For inorganic secondary aerosols (SPM), residual scatter is greater (standard error of 1.2). With the only exception of the iF comparison for nitrates with the study by Levy, Wolff et al., 2002 (US national-level estimate), intake factors agree within a factor of two. The mean fractional bias is +7.6% (UWM underestimates).

Tab.8. Pollutant intake factors for US and China (parts per million, ppm)

Pollutant	UWM (Eqns.7 and 17)			CALPUFF iF [ppm]	
	k [cm/s]	iF [ppm]	68% CI	mean	Low-High
Study¹: Beijing, China (Zhou et al., 2003); $\rho_{\text{eff}} = 213 \text{ pers/km}^2$ and $S_{\text{ct}} = 1$					
PPM _{2.5}	0.43	11.6 (15.5)	7 – 16 (10 – 23)	15	9 – 25
Sulfates	1.77	2.8	1.7 – 3.9	6.0	3 – 11
Nitrates	0.82	6.0	3.7 – 8.3	6.5	2 – 15
Study²: 29 sites in China (Zhou et al., 2006); $\rho_{\text{eff}} = 231 \text{ pers/km}^2$ & $S_{\text{ct}} = 0.5$ (nitrates)					
PPM _{2.5}	0.69	7.7	4.7 – 11	6.1	1.7 – 12
Sulfates	2.14	2.5	1.5 – 3.5	4.4	0.73 – 7.3
Nitrates	0.96	2.8	1.7 – 3.9	3.5	0.80 – 7.1
Study³: 9 sites in Illinois, USA (Levy, Spengler et al., 2002); $\rho_{\text{eff}} = 60 \text{ pers/km}^2$ & $S_{\text{ct}} = 0.5$ (nitrates)					
PPM _{2.5}	0.37	2.3	1.4 – 3.2	2.1	0.6 – 4
Sulfates	1.96	0.42	0.26 – 0.59	0.26	0.1 – 0.3
Nitrates	0.99	0.42	0.23 – 0.51	0.36	0.16 – 0.4
Study⁴: 40 sites in the USA (Levy, Wolff et al., 2002); $\rho_{\text{eff}} = 32 \text{ pers/km}^2$ & $S_{\text{ct}} = 0.5$ (nitrates)					
PPM _{2.5}	0.37	2.0	1.2 – 2.8	2.2	0.25 – 6.3
Sulfates	1.96	0.38	0.23 – 0.53	0.22	0.083 – 0.3
Nitrates	0.99	0.092	0.23 – 0.51	0.035	0.0096 – 0.075

Tab.8 Footnotes

1. For the Beijing case study, two $\text{PPM}_{2.5}$ iF estimates have been calculated: (i) using Eqn.7 with default data shown in the table and (ii) an improved estimate in which the modeling domain has been subdivided into local and regional areas. At the local-level (Beijing municipality), the mean concentration was evaluated using Eqn.11, where R_o (73 km) is the effective radius of the municipality area (1167 km^2) and $4000 \text{ m}^2/\text{s}$ was used for the dilution rate. The incremental concentration was multiplied by the population (19.6 million people) to obtain the collective exposure and by the mean daily breathing rate ($20 \text{ m}^3/\text{pers}$) to determine the (local) intake fraction (4.76 ppm). Eqn.10a was used to compute the regional intake, integrating from $r = R_o$ to ∞ (10.7 ppm).

2. For the Chinese national-level calculations, the depletion velocities are population weighted averages for the whole of China. These values are bit different, understandably, than those reported in Tab.4 because of differences in the normalized areas. Estimates for nitrates have been scaled by 50% to account for the non-linear chemical transformation of precursor NO_x emissions (Tab.1).

3. In the Levy, Spengler et al., (2002) study, the intake factor was evaluated over an impact radius of 400 to 500 km. Based on Figs. 4 and 5 (or Eqn.15 with $\rho_{\text{loc}} = 88$ and $\rho_{\text{back}} = 59 \text{ pers}/\text{km}^2$), the UWM estimates have been scaled by 60% to account for the smaller impact range. It is worth noting that the data in these figures are consistent with the profiles shown in Fig.2 in Zhou et al., (2003).

4. The UWM results for nitrates have been divided by four to be consistent with the hypothesis in Levy, Wolff et al., (2002) that postulates that nitrates formation only happens during the wintertime. Although it is certainly true that nitrate formation is significantly reduced during the warmer month (Zhou et al., 2003 and Tarrasón et al., 2004), dividing the annual concentration by four may lead to underestimation of the annual intake factor (see, for example, Table 2 in Zhou et al., 2003 and Figure 5.8 in Tarrasón et al., 2004).

5. Finally, it should be noted that CALPUFF estimates may be significantly influenced by modeling assumptions, grid resolution and choice of default input data and meteorology. According to a validation study by the US EPA (1998b), CALPUFF simulated results were within a factor of two of observed data, with no consistent over- or under-prediction. Annual predictions tend to be better correlated with measured data than monthly averages (IES 2005a). Zhou et al., (2003) have considered several sensitivity analyses to test the variability and uncertainty of intake factors to CALPUFF input data. Hao et al., (2007) estimated intake factors for power plant emissions (primarily coal generation) in the metropolitan area of Beijing (180 by 184 km, with grid resolution 4 by 4 km) using the CALPUFF model. According to their analysis, there was a factor of two difference between their results for local iF estimates and the data presented in Zhou et al., (2003), who used a resolution grid spacing of 28 by 28 km. Choice of power plants included in the analysis and source-receptor distances may explain some of the difference between these two studies. Grid resolution influences may also explain why there is only a factor of four difference between iF factors for mobile sources compared to stationary sources in Levy, Wolff et al., (2002), who assumed a grid size 100 by 100 km. This factor is at least ten for typical cities (HEATCO 2006).

4.6. Impact of Power Generation on Air Quality in Beijing (China)

Objective: The objective of this analysis is to apply the UWM to compute for Beijing the influence on air quality from power sector PPM_{10} emissions. Mean urban concentration is computed using Eqn.11 and compared with results from the Integrated Environmental Strategies (IES) program. The IES program is a collaborative venture between US academic and research institutions and international partners with the aim to identify, evaluate through a cost-benefit analysis and eventually inform policymakers about pollutant emission control options that can improve local air quality, and consequently realize public health benefits from reduced local pollutant concentrations, and at global level achieve the co-benefit of lower emissions of greenhouse gases. The IES-China program is a US-China consortium of participants, including the National Renewable Energy Laboratory (NREL) and School of Public Health at Yale University on the US side and the Department of Environmental Science, Tsinghua University and School of Public Health at Peking University on the Chinese side.

Input data and results: Assessment input data and comparison of UWM output with results from the IES program (IES 2005a) are shown in Tab.9. The incremental concentration is the arithmetic mean across the Beijing metropolitan area, not the population weighted average, for aggregated power sector PM_{10} emissions for the business as usual (BAU) scenario in 2010. As can be seen in Fig.18 (Hao et al., 2007), the most damaging power plants are located close to the outer edges of the city (shaded area). Consequently, the second UWM estimate, corresponding to an effective radius R_0 of 47.6 km, is considered a more robust (realistic) concentration estimate for the present situation. A weighted average of the UWM estimates, assuming a 2:1 weighting factor in favor of the second concentration estimate gives $0.62 \mu\text{g}/\text{m}^3$, which is within 25% of the ISC3 (short-term) result reported in the IES document. The UWM 68% confidence interval was computed assuming a lognormal concentration distribution with σ_g of 1.5. The composite probability function of the sum of two lognormal functions was obtained using the technique suggested in Spadaro and Rabl (2008).

The comparison between UWM and ISC3 mean concentrations is quite reasonable, and is not entirely unexpected considering the good agreement already noted in Fig.10 for tall stack emissions near the city of Paris in France. It follows, therefore, that health impacts, both in physical units (cases) and in terms of economic costs would also compare favorably between the UWM approach and the ISC based analysis. In the original IES study, CRFs and unit cost are summarized in Chapter 6 (Tabs.6.2 and 6.4) and in Chapter 7 (Tab.7.2). The market price of CO_2 emissions was set to 12\$/ton. Superimposing population and concentration spatial profiles would yield a population-weighted average exposure. It is this mean estimate that would be multiplied by the sum of the products of concentration-response functions and unit costs per health endpoint to obtain the local social cost (Eqn.8). The overall damage cost is the sum of local and regional contributions. The regional contribution comes to 45% of the total, according to Eqn.15 with $\frac{\rho_{loc}}{\rho_{back}} = \frac{6447}{213} = 30$, $R_{loc} = 24$ km and $\lambda_p = 0.0016 \text{ km}^{-1}$. This is a little less than the local effect, entirely consistent with the profiles in Fig.4.

Tab.9. Influence of power sector PPM_{10} emissions on urban air quality in Beijing, China

UWM calculation details for BAU 2010		
Power sector emissions	9,000 t/yr (Tab.4.8, IES 2005a report)	Q_p
Beijing inner city zone		
■ Urban area	1,782 km ² (p.38 in IES report)	
■ Equivalent radius of urban area	23.8 km	
■ Urban population	11,488,000 persons (p.83, IES report)	6,447 pers/km ²
UWM input data		
■ Depletion velocity	0.64 cm/s	$u = 5 \text{ m/s}, h_{\text{mix}} = 800 \text{ m}$
■ Dilution rate	4,000 m ² /s	$\lambda_p = 1.6E-6 \text{ m}^{-1}$
UWM mean concentration (Eqn.11)		<see text for details>
■ Power plants inside city	0.94 $\mu\text{g}/\text{m}^3$ ($R_o = 23.8 \text{ km}, \sigma_g = 1.5$)	Central estimate: 0.62 $\mu\text{g}/\text{m}^3$
■ Power plants along city edge	0.46 $\mu\text{g}/\text{m}^3$ ($R_o = 47.6 \text{ km}, \sigma_g = 1.5$)	68% CI: 0.44 – 0.79 ($\sigma_g = 1.34$)
IES 2005a study (ISC3 Short-term dispersion model used to asses air quality changes, EPA 1995)		
ISC3 mean concentration	0.5 $\mu\text{g}/\text{m}^3$ (Tab.5.4 in report)	$\pm 10\text{-}15\%$ uncertainty (Fig.5.6)



Fig.18. Locations of fossil fuel power plants in Beijing, China. The Beijing metropolitan area is distinguished from the rest of the Beijing Municipality by the gray shaded area. Combined emissions from Jingfeng, Datang and Jingneng plants contributed to more than 70% of total PM_{10} power emissions in 2000, while Huadian’s contribution was only 5%. (Ref: Hao et., 2007)

4.7. Influence of Transport Emissions on Air Quality in Hyderabad (India)

Objective: As a final comparison, the mean ground-level concentration change attributable to PPM_{10} transport emissions will be predicted using a slightly modified form of the uniform world model methodology that has been adapted to the case of ground-level sources. The UWM estimate will then be compared with results from the IES-India program (IES 2005b). The city of Hyderabad, the 5th largest city in India, has been selected for this exercise. Just like the IES-China study for Beijing, the co-benefits analysis of the Hyderabad Urban Development Area (HUDA) study focuses on developing an analytical framework for quantifying industrial and transport emissions inventories and assessing the costs and benefits of clean energy strategies aimed to protect public health and reduce emissions of greenhouse gases. The HUDA study was carried out by the Environment Protection Training and Research Institute in Hyderabad, with technical guidance provided by the USEPA, NREL and other international groups. A copy of the final report (more than 400 pages) may be downloaded from <http://www.epa.gov/ies/india/index.htm>.

Input data and results: For an elevated emission source (ELS), Eqn.11 provides an estimate of the mean ambient concentration over the range 0 to R_o . However, this equation in its present form is inadequate to model ground-level (mobile) emission sources (GLS). Two corrections are proposed. First, the exponential term inside the square brackets in Eqn.11 is set to (*approximately*) zero. This is a modeling construct that is equivalent to reducing the mixing height (h_{mix}) to near ground level. A smaller mixing depth reduces atmospheric dilution, “trapping” the pollution, and consequently the plume centerline remains closer to the ground. This is indeed the case for transport emissions. Second, adjust for the low stack height of transport emissions using the S_{sh} multiplier for small plume rise that was given in Eqn.12. h_s is the source physical stack height, taken as 10 meters in this example (incidentally, 10 m is the typical height at which wind speed is recorded). Once again, this is a modeling construct to indicate the downwind “effective” plume centerline for transport emissions.

Eqn.18 below is the proposed relationship for predicting the mean ambient concentration from mobile (ground-level) emissions. The length of any road segment should be kept to a maximum of 10 to 15 km. Half of this value represents the value of R_o , this is the radius of a circular area centered at the midway point along the road. The population weighted exposure is the product of the concentration computed with Eqn.18 and the number of people exposed within the circle.

$$\bar{C}_p^{Transport}(R_o) \approx S_{sh} \left[\frac{Q_p}{\pi k_p R_o^2} \right] = \left(\frac{20}{h_s^{0.49}} \right) \left[\frac{Q_p}{\pi k_p R_o^2} \right] \quad (18)$$

Input data, UWM prediction and comparison with ISC3 (short-term model) are summarized in Tab.10. A map of the HUDA study area showing locations of industrial and transport emissions is shown in Fig.19. As seen in Tab.10, the UWM correctly predicts the order of magnitude of the mean

urban concentration, and its absolute value is within 20% of the ISC estimate. For current conditions, the exponential factor set to zero in Eqn.11 has a value of 0.1 (the local wind speed u is 3.3 m/s; cf. Annex C, p.254). A factor not considered here is the street canyon effect, which could conceivably increase the final estimate of the total damage cost by between 50% and 100%.

As a final observation, industrial emissions have a negligible effect on urban concentrations, whereas transport emissions have a major implication on local air quality. The Indian National Ambient Air Quality Standards (NAAQS) for PM_{10} are $100 \mu\text{g}/\text{m}^3$ and $60 \mu\text{g}/\text{m}^3$, respectively, for the 24-hour and annual average; both standards are exceeded in Hyderabad. Consequently, policy options for controlling mobile emissions must be a priority.

Tab.10. Influence of transport sector PPM_{10} emissions on urban air quality in Hyderabad, India

UWM calculation for the Hyderabad District (MCH), BAU 2001		
Hyderabad District <ul style="list-style-type: none"> ■ Urban area ■ Equivalent radius of urban area ■ Urban population 	173 km ² (Annex C, p.93) 7.4 km 3,633,000 persons (Annex C, p.93)	IES-2005b (India) R _o (size of HUDA is 24.6 km) 21,049 pers/km ² (3,350 pers/km ² for HUDA)
UWM input data <ul style="list-style-type: none"> ■ Depletion velocity ■ Dilution rate (Industrial emissions) 	1 cm/s 4,000 m ² /s	k _p u = 5 m/s, h _{mix} = 800 m λ _p = 2.5E-6 m ⁻¹
<u>Industrial sector</u> <ul style="list-style-type: none"> ■ Annual emissions ■ UWM concentration 	1,187 t/yr 0.07 μg/m ³	Annex A, p.57 Industrial sources are located outside of the city, 10-20 km. Integrate Eqn.10a for r between 10 and 20 km.
<u>Transport sector</u> <ul style="list-style-type: none"> ■ Annual emissions ■ UWM concentration (Eqn.18) 	1,825 t/yr (total PPM_{10} for HUDA) 131 μg/m³	5 tons daily (Annex C, p.187); assume 60% occur within MCH Q _p = 1,100 t/yr, h _s = 10 m
IES 2005b study (ISC3 Short-term dispersion model used to asses air quality changes, EPA 1995)		
ISC3 mean concentration	160 μg/m³	Tab.2, p.72 (Annex B)

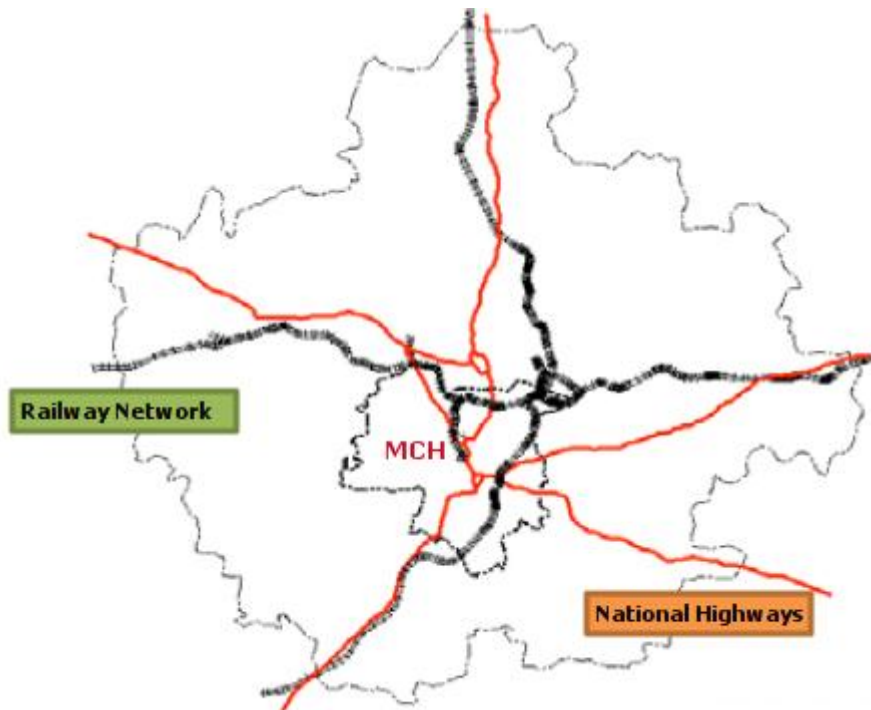
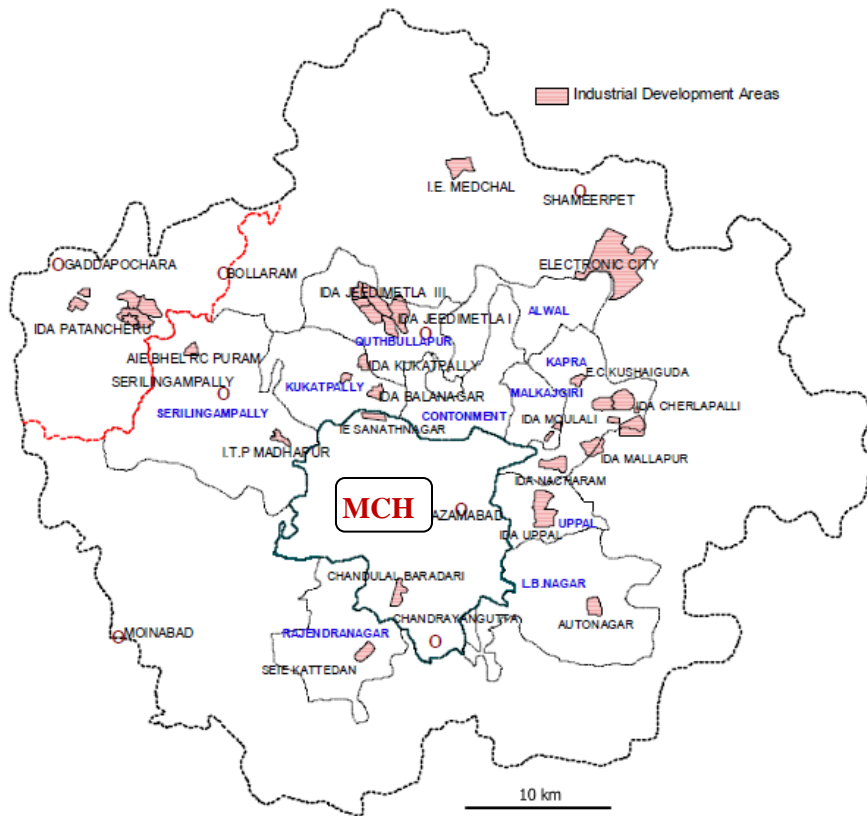


Fig.19. Hyderabad Urban Development Area (HUDA) showing the location of the Hyderabad District (MCH), industrial sources (top) and main transport emission corridors (bottom). (Ref: IES 2005b)

5. Concluding Remarks

The scope of the present work has been to present a simple and convenient environmental impact assessment tool, the Uniform World Model (UWM), which can provide estimates of the adverse consequences to public health following inhalation exposure to routine atmospheric emissions. The model is a product of a few factors; it is simple and transparent, showing at a glance the role of the most important parameters of the impact pathway analysis. If all the parameters are geographically uniform, it is exact, as consequence of the conservation of mass. It is also exact for tall stacks in the limit where the distribution of either the sources or the receptors is uniform and the key atmospheric parameters do not vary with location.

The UWM has been compared with results from detailed impact assessments that have been carried out in Europe, China, India and the USA, and in all instances its outcome has been found to be quite “robust”, with usual deviations well within the $\pm 50\%$ range. Rural, regional or continental estimates are more accurate than site specific case studies for large urban areas, but suitable correction factors can be used to improve agreement with results from detailed models, even in the case for transport emissions (Tab.1). For a typical city and a source physical stack height greater than 25 m, the UWM estimate, as computed by Eqn.8, is usually within a factor of two or three. For stacks in excess of 200 meters, even in the proximity of large cities, the ground-level near field mean concentration (< 50 km) is often well within $\pm 50\%$ (Fig.10).

The reason why the UWM is such a good representation of typical results is that averaging over many sites is equivalent to averaging over different distributions of population, thus rendering the distribution more uniform. The UWM involves the replacement of the average of a product by the product of the averages, an approximation that is justified to the extent that the factors are not correlated with each other and do not vary too much. In practice, the concentration varies the most, being high near the source and decreasing with downwind distance r as $\frac{e^{-\lambda r}}{r}$. For sources close to or inside large cities, this variation is correlated with the population density and so the UWM, understandably, underestimates the impact. For sources far from large cities, the strong spatial variation of population density occurs in a region where the concentration varies slowly, consequently taking the mean population density is adequate and the UWM prediction is acceptable.

In conclusion, the UWM has the advantage of providing typical values of concentrations and intake factors and typical estimates of human health impacts and social damage costs of air pollution that can be effectively used to assess the benefits of pollutant emission control technologies or policy strategies legislated at the regional-, country- or sector-specific level and that contribute to improving local, regional or global air quality and reducing greenhouse gas emissions.

6. Further Reading

Amann, M, Kejun, J, Jiming, H and others. 2008. *GAINS-ASIA, Scenarios for Cost-Effective Control of Air Pollution and Greenhouse Gases in China*. IIASA, Schlossplatz 1, Laxenburg, 2361, Austria.

Cohen, A, Anderson, R, Ostro, R, Pandey, KD, Kryzanowski, M, Kunzli, N, Gutschmidt, K, Pope, A, Romieu, I, Samet, J and Smith, K. 2004. Mortality Impacts of Air Pollution in the Urban Environment. In *Comparative Quantification of Health Risks: Global and Regional Burden of Diseases due to Selected Major Risk Factors*, Ezzati, M, Lopez, AD, Rodgers, AD and Murray, CJL, Editors. World Health Organization, Geneva.

Curtiss, P and Rabl, A. 1996. Impacts of Air Pollution: General Relationships and Site Dependence. *Atmospheric Environment*, **30**:3331-3347.

EEA 2011. European Environment Agency. *Revealing the Costs of Air Pollution from Industrial Facilities in Europe*. EEA Technical Report No 15/2011, ISSN 1725-2237, Nov 2011.

EPA 2011. Environmental Protection Agency. *Exposure Factors Handbook: 2011 Edition*. Office of Research and Development, Washington, DC 20460, USA. EPA/600/R-090/052F, Sep 2011.

EPA 1998a. *A Comparison of CALPUFF with ISC3*. Office of Air Quality, Planning and Standards, Research Triangle Park, NC, USA. EPA-454/R-98-020, Dec 1998.

EPA 1998b. *A Comparison of CALPUFF modeling Results to Two Tracer Field Experiments*. Office of Air Quality, Planning and Standards, Research Triangle Park, NC, USA. EPA-454/R-98-009, Jun 1998.

EPA 1995. *User's Guide for the Industrial Source Complex (ISC3) Dispersion Models*, Volumes I - III. EPA-454/B-95-003a-c. (<http://www.epa.gov/scram001/userg/regmod/isc3v1.pdf>). Details about the ISC model are found on the EPA's website http://www.epa.gov/ttn/scram/dispersion_alt.htm#isc3.

Hao, J, Wang, L, Shen, M, Li, L and Hu, J. 2007. Air Quality Impacts of Power Plant Emissions in Beijing. *Environmental Pollution*, **147**:401-408.

Health Effects Institute (HEI). 2010. *Outdoor Air Pollution and Health in the Developing Countries of Asia; A Comprehensive Review, Special report 18*. Health Effects Institute, Boston, MA, USA, Nov 2010.

HEATCO 2006. Developing Harmonised European Approaches for Transport Costing and Project Assessment. Deliverable 5: Proposal for Harmonized Guidelines. European Commission, FP6 Programme Contract #FP6-2002-SSP-1/502481.

IES 2005a. Integrated Environmental Strategies, *Energy Options and Health Benefit – Beijing Case Study*. Report prepared by NREL, USA, Department of Environmental Science, Tsinghua University, China, School of Public Health, Peking University, China and School of Public Health, Yale University, USA, Nov. 2005. IES Program http://www.epa.gov/ies/china/national_assessment.html.

IES 2005b. *Project in Hyderabad, India: Co-Benefits Analysis of the Hyderabad Urban Development Area*. Report prepared by the Environment Protection Training and Research Institute, Hyderabad-500032, India, April 2005. IES Program <http://www.epa.gov/ies/india/index.htm>.

Kalantzi, EG, Makris, D, Duquenne, MN, Kaklamani, S, Stapountzis, H and Gourgoulianis, KI. (2011). Air Pollutants and Morbidity of Cardiopulmonary diseases in a Semi-Urban Greek Peninsula. *Atmospheric Environment*, **45**:7121-7126.

Khoder, MI. 2002. Atmospheric Conversion of Sulfur Dioxide to Particulate Sulfate and Nitrogen Dioxide to Particulate Nitrate and Gaseous Nitric Acid in an Urban Area. *Chemosphere*, **49**:675-684.

Lee and Watkiss. 1998. Working paper for the ExterneE Project of the European Commission.

Levy, J, Spengler, JD, Hlinka, D, Sullivan, D and Moon, D. 2002. Using CALPUFF to Evaluate the Impacts of Power Plant Emissions in Illinois: Model Sensitivity and Implications. *Atmospheric Environment*, **36**:1063-75.

Levy, J, Wolff, SK and Evans, JS. 2002. A Regression-Based Approach for Estimating Primary and Secondary Particulate Matter Intake Fractions. *Risk Analysis*, **22**(5):895-904.

Luhar, AK. 1998. An Analytical Slab model for the Growth of the Coastal Thermal Internal Boundary Layer under Near-Neutral Onshore Flow Conditions. *Boundary-Layer Meteorology*, **88**:102-120.

Luria, M, Imhoff, RE, Valente, RJ, Parkhurst, WJ and Tanner, RL. 2001. Rates of Conversion of Sulfur Dioxide to Sulfate in a Scrubbed Power Plant Plume. *Journal Air Waste Management Assoc*, **51**:1408-1413.

Miyakawa, T, Takegawa, N and Kondo, Y. 2007. Removal of Sulfur Dioxide and Formation of Sulfate Aerosol in Tokyo. *Journal of Geographical Research*, **112**, D13209.

Pope, CA III, Burnett, RT, Turner, MC, Cohen, A, Kreswski, D, Jerrett, M, Gapstur, SM and Thun, MJ. 2011. Lung Cancer and Cardiovascular Disease Mortality Associated with Ambient Air Pollution and Cigarette Smoke: Shape of the Exposure-Response Relationships. *Environmental Health Perspectives*, <http://dx.doi.org/10.1289/ehp.1103639>. July 2011.

- Pope, CA III, Burnett, RT, Krewski, D, Jerrett, M, Shi, Y, Calle, EE and Thun, MJ. 2009. Cardiovascular Mortality and Exposure to Airborne Fine Particulate Matter and Cigarette Smoke: Shape of the Exposure-Response Relationship. *Circulation*, **120**:941-948.
- Pope, CA III, Burnett, RT, Thurston, GD, Thun, MJ, Calle, EE, Krewski, D, Godleski, JJ. 2002. Cardiovascular Mortality and Long-Term Exposure to Particulate Air Pollution: Epidemiological Evidence of General Pathophysiological Pathways of Disease. *Circulation*, **109**:71-77.
- Rabl, A and Spadaro, JV. 1999. Damages and Costs of Air Pollution: An Analysis of Uncertainties. *Environment International*, **25**(1):29-46.
- Scire JS, Strimaitis DG, Yamartino RJ. 2000. *A user's guide for the CALPUFF dispersion model (Ver 5)*. Earth Tech Inc.; 2000.
- Seinfeld JH and Pandis, SN. 1998. *Atmospheric Chemistry and Physics: From Air Pollution to Climate Change*, John Wiley & Sons, Inc., New York, USA.
- Spadaro, JV and Rabl, A. 2008. Estimating the Uncertainty of Damage Costs of Pollution: A Simple Transparent Method and Typical Results. *Environmental Impact Assessment Review*, **28**:166-183.
- Spadaro, JV and Rabl, A. 2005. Dispersion Models for Time-Averaged Collective Air Pollution exposure: An Estimation of Uncertainties. Centre Energétique et Procédés, Ecole des Mines (ARMINES), 60 Boulevard St. Michel, Paris, France.
- Spadaro, JV. 1999. Quantifying the Damages of Airborne Pollution: Impact Models, Sensitivity Analyses and Applications. Ph.D. Doctoral Thesis, Ecole des Mines de Paris, Boulevard St. Michel, 60, Paris Cedex 06, F75272
- Tarrasón, L, Fagerli, H, Jonson, JE, Klein, H, van Loon, M, Simpson, D, Tsyro, S, Vestreng, V and Wind, P. 2004. Transboundary Acidification, Eutrophication and Ground Level Ozone in Europe. EMEP/MS-C-W, Norwegian Meteorological Institute, EMEP Status Report 2004, ISSN 0806-4520.
- West, JJ, Ansari, AS, Pandis, SN. 1999. Marginal PM_{2.5}: nonlinear aerosol mass response to sulfate reductions in the eastern United States. *Journal of the Air and Waste Management Association* **49**:1415-1424.
- Zannetti, P. 1990. *Air Pollution Modeling. Theories, Computational Methods and Available Software*, Van Nostrand-Reinhold.
- Zhou, Y, Levy, JI, Evans, JS and Hammitt, JK. 2006. The Influence of Geographic Location on Population Exposure to Emissions from Power Plants throughout China. *Environment International*, **32**:365-373.

Zhou, Y, Levy, JI, Hammitt, JK, Evans, JS. 2003. Estimating Population Exposure to Power Plant Emissions using CALPUFF: A Case Study in Beijing, China. *Atmospheric Environment*, **37**:815-826.

BC3 WORKING PAPER SERIES

Basque Centre for Climate Change (BC3), Bilbao, Spain

The BC3 Working Paper Series is available on the internet at the following addresses:

http://www.bc3research.org/lits_publications.html

<http://ideas.repec.org/s/bcc/wpaper.html>

BC3 Working Papers available:

- 2010-15 Karen Pittel and Dirk Rübbelke: *Local and Global Externalities, Environmental Policies and Growth*
- 2010-16 Margherita Grasso, Matteo Manera, Aline Chiabai, and Anil Markandya: *The Health Effects of Climate Change: A Survey of Recent Quantitative Research*
- 2010-17 Luis Mari Abadie, Ramon Arigoni Ortiz and Ibon Galarraga: *The Determinants of Energy Efficiency Investments in the U.S.*
- 2011-01 Roger Fouquet: *Long Run Trends in Energy-Related External Costs*
- 2011-02 Dirk Rübbelke: *International Support of Climate Change Policies in Developing Countries: Strategic, Moral and Fairness Aspects*
- 2011-03 Melanie Heugues: *Endogenous Timing in Pollution Control: Stackelberg versus Cournot-Nash Equilibria*
- 2011-04 Karen Pittel and Dirk Rübbelke: *International Climate Finance and its Influence on Fairness and Policy*
- 2011-05 Wan-Jung Chou, Andrea Bigano, Alistair Hunt, Stephane La Branche, Anil Markandya, Roberta Pierfederici: *Households' WTP for the Reliability of Gas Supply*
- 2011-06 Roger Fouquet and Peter J.G. Pearson: *The Long Run Demand for Lighting: Elasticities and Rebound Effects in Different Phases of Economic Development*
- 2011-07 Ibon Galarraga, David Heres Del Valle and Mikel González-Eguino: *Price Premium for High-Efficiency Refrigerators and Calculation of Price-Elasticities for Close-Substitutes: Combining Hedonic Pricing and Demand Systems*
- 2011-08 Anil Markandya, Mikel González-Eguino, Patrick Criqui, Silvana Mima: *Low Climate Stabilisation under Diverse Growth and Convergence Scenarios*
- 2011-09 Martin Altemeyer-Bartscher, Anil Markandya and Dirk Rübbelke: *The Private Provision of International Impure Public Goods: the Case of Climate Policy*
- 2011-10 Aline Chiabai, Ibon Galarraga, Anil Markandya and Unai Pascual: *The Equivalency Principle for Discounting the Value of Natural Assets: An Application to an Investment Project in the Basque Coast*
- 2011-11 Roger Fouquet: *The Demand for Environmental Quality in Driving Transitions to Low Polluting Energy Sources*
- 2011-12 Joseph V. Spadaro: *The Uniform World Model: A Methodology for Predicting the Health Impacts of Air Pollution*